Recent Progress in Substrate-Transferred Crystalline Mirrors

Garrett D. Cole

Vienna Center for Quantum Science and Technology

Outline

- Brownian noise and crystalline multilayer motivation
  - applications, crystal growth, and basic properties
- Confirmation of high reflectivity and low loss angles
  - damping and thermal noise in micro- and meso-scale mirrors
- Crystalline mirrors for precision measurement
  - bonded “macroscopic” mirrors for optical reference cavities
- Path towards low-thermal-noise LIGO-scale mirrors
  - exploit existing infrastructure for IC fabrication

Different Scale, Similar Requirements

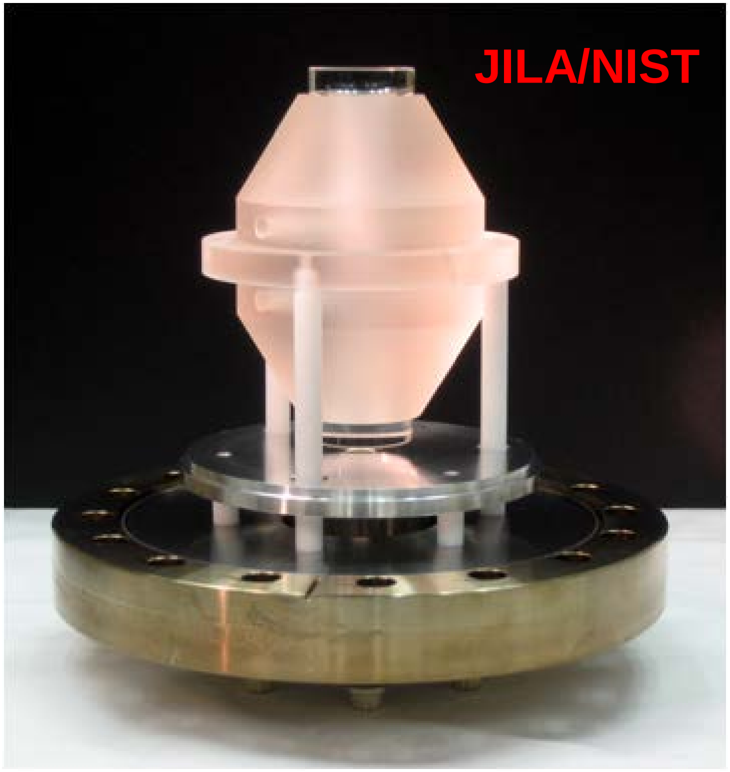

- Brownian noise poses a significant hurdle for a number of endeavors
  - micro- and nanoscale scale resonators for cavity optomechanics
  - reference cavities for laser stabilization (optical atomic clocks, freq. comb)
  - kilometer-length gravitational wave interferometers

Coating Thermal Noise Basics

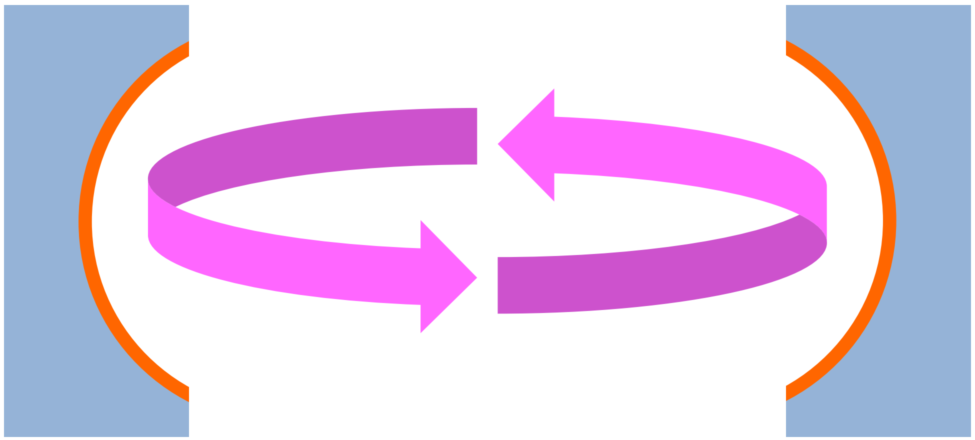

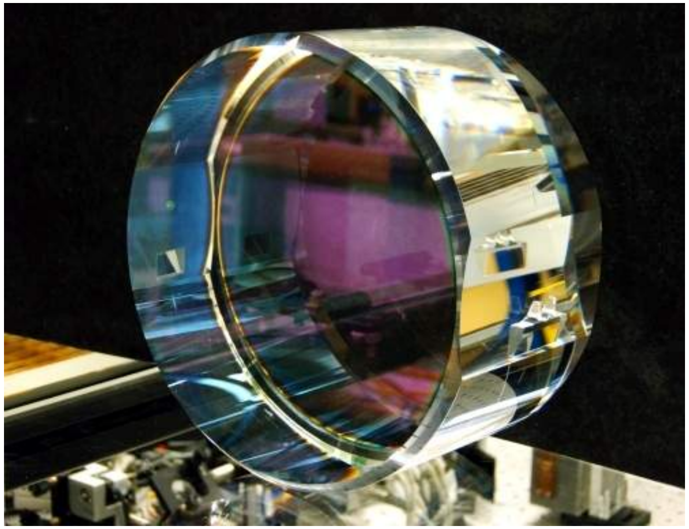

- Mirrors are limiting factor in high-stability resonator performance
  - not optical, but rather poor mechanical properties of the mirror
- Excess mechanical damping in multilayer leads to significant noise
  - dissipation: coupling of mechanical motion to a heat reservoir
  - mechanical loss → thermal fluctuations → mechanical fluctuations

Coating Thermal Noise Consequences

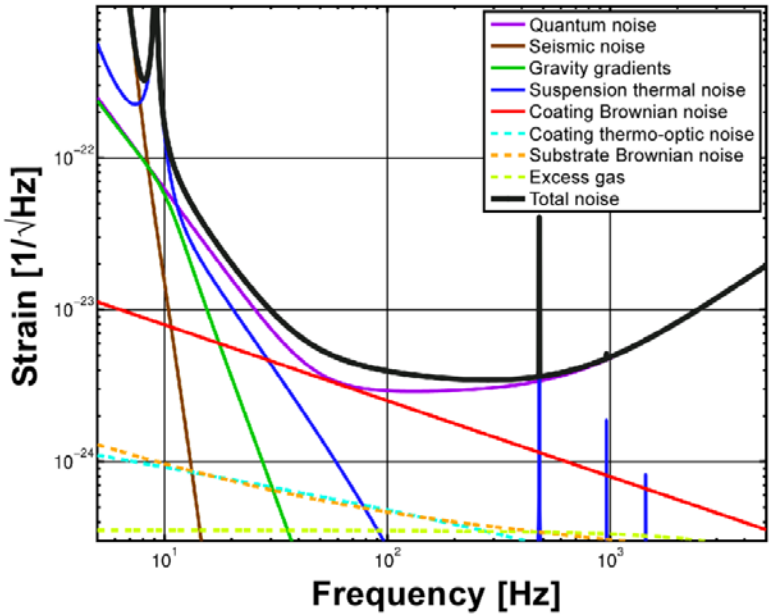

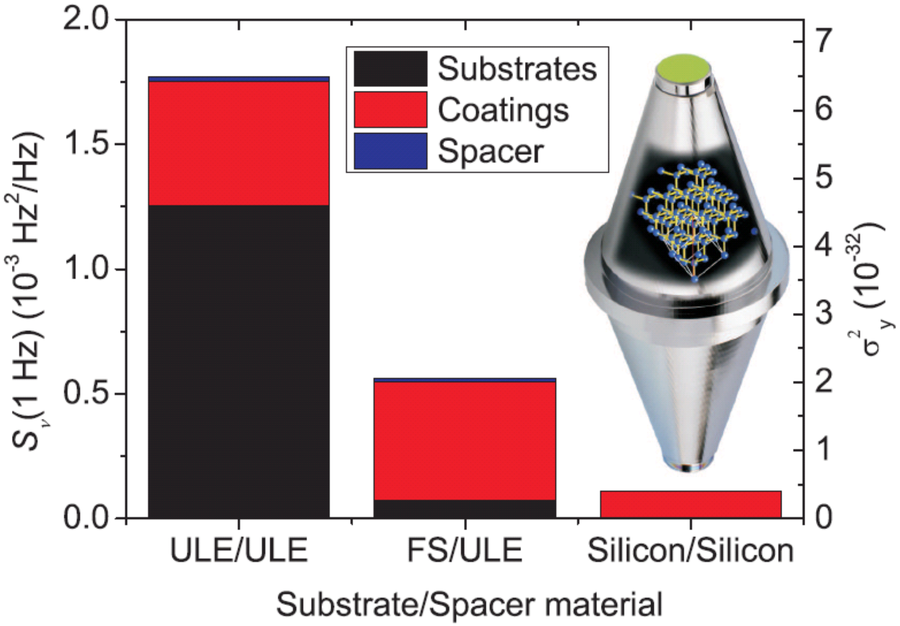

- State-of-the-art systems now limited by dielectric multilayer mirrors
  - from LIGO-relevant studies by Penn, Harry, etc. Ta_2O_5 is the culprit
  - only incremental changes realized in the last decade
- Completely new solution is required here – *crystalline coatings!*
  - semiconductor industry has a long history with such materials systems

Kessler, Hagemann, Grebing, Legero, Sterr, Riehle, Martin, Chen, Ye, arXiv:1112.3854v2

Optomechanics: Sculpted DBRs

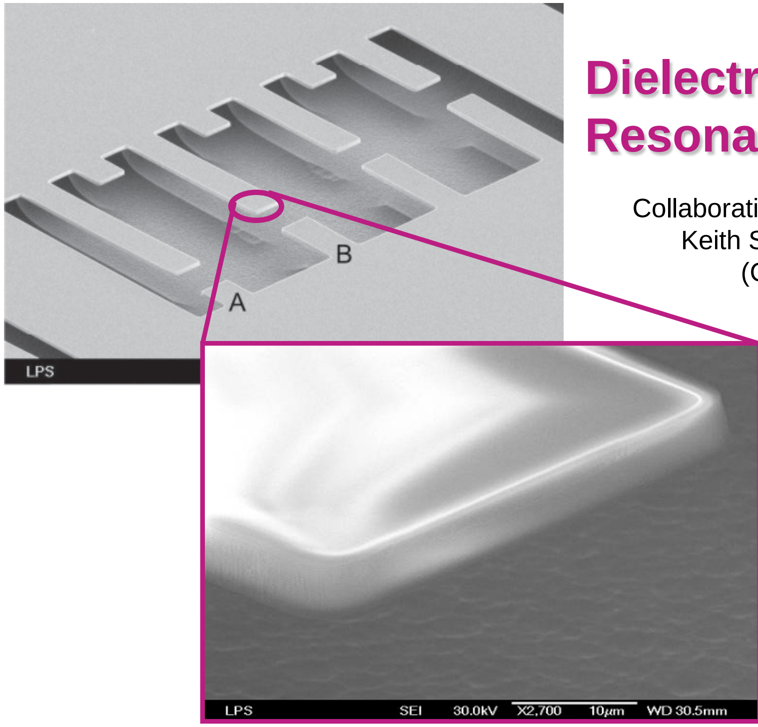

Dielectric Resonators

Collaboration with
Keith Schwab
(Cornell)

free-standing Ta_2O_5/SiO_2 HR coating

Reflectivity > 0.9999, Q ~ 2000 – 6000

loss angle (Q^{-1}) similar to LIGO data

S. Gröblacher, S. Gigan, H. Böhm, A. Zeilinger, M. Aspelmeyer, Eur. Phys. Lett. 81, 54003 (2008)

Epitaxial AlGaAs Bragg Mirrors

FBH and Aspelmeyer
Group (UniVie)

free-standing epitaxial AlGaAs DBR

Reflectivity > 0.9999, Q ~ 2×10^4 – 2×10^5

Significantly reduced damping, similar R

a) Cole, et al., Appl. Phys. Lett. 92, 261108 (2008)

b) Cole, et al., Appl. Phys. Lett. 96, 261102 (2010)

Multilayer Details

- AlGaAs multilayer with varying Al content for index contrast
  - high index layers contain low Al content (0-12%)
  - 8% Ga incorporated in low index film to slow oxidation in ambient
- High quality epitaxy requires a lattice matched substrate
  - same crystalline symmetry
  - minimal deviation of lattice parameter (atomic spacing)
- Potential for high reflectivity from ~600 nm – 3 μm
  - measurements @ 1064 nm

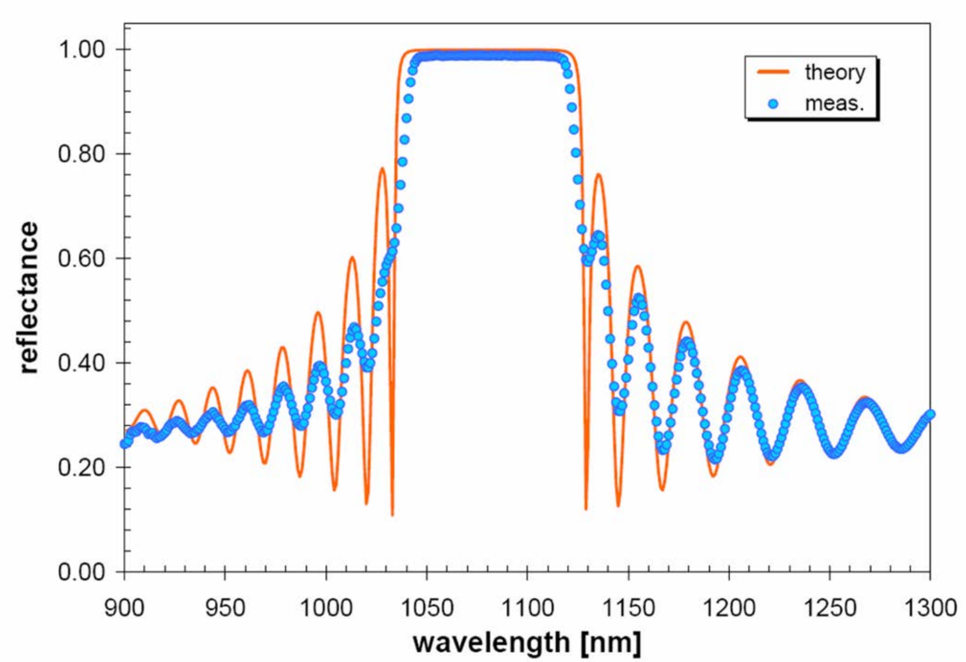

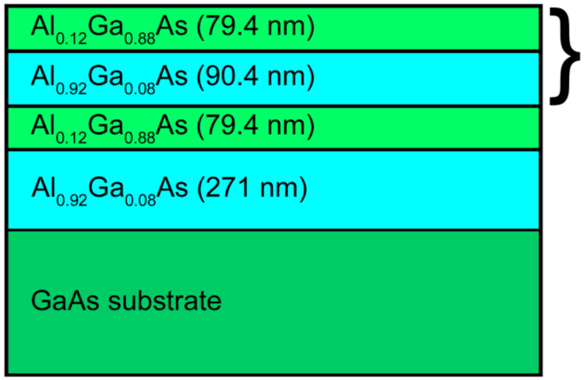

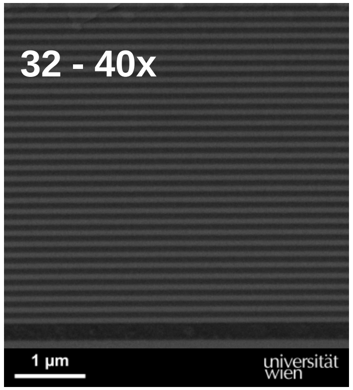

G. D. Cole, et al., Appl. Phys. Lett. 92, 261108 (2008)

Crystal Growth Techniques

molecular beam epitaxy

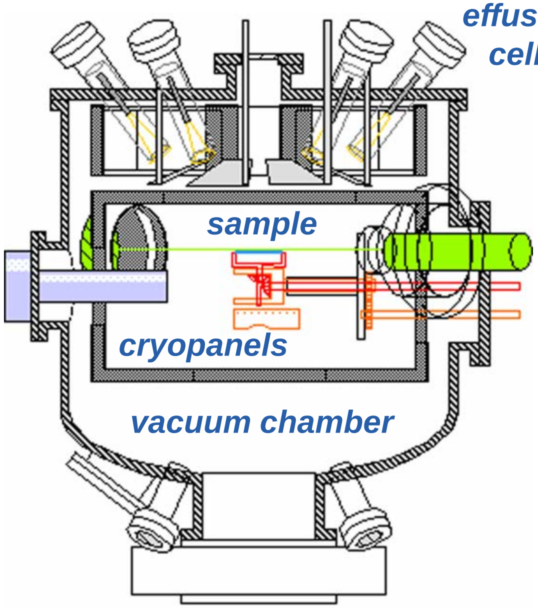

metal organic chemical vapor deposition

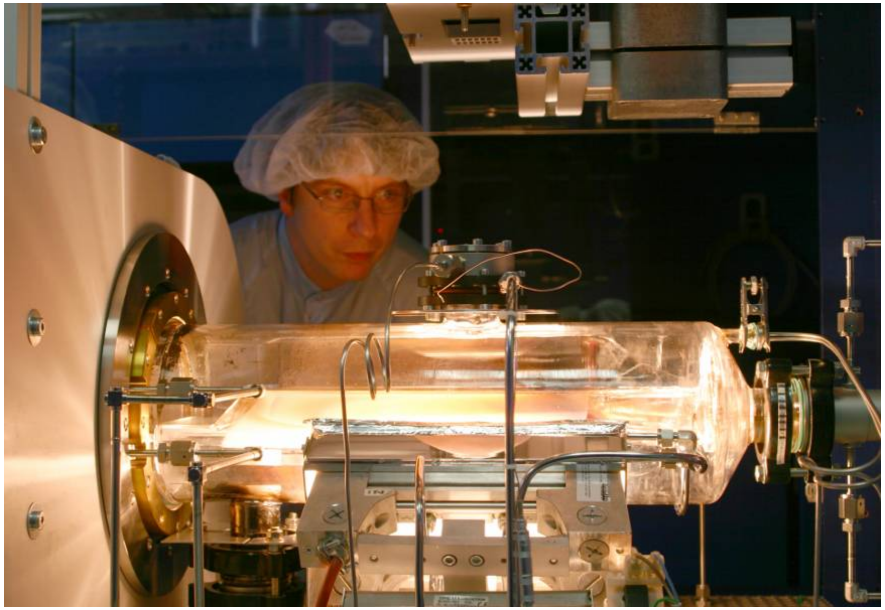

Material	Crystal structure	Lattice const. (A)	Modulus ($GPa_{\|\|,\perp}$)	Density (kg/m^3)	CTE ($x10^{-6}\ K^{-1}$)	Index (1064 nm)
GaAs	zinc blende	5.6455	85.3/121.3	5320	5.73	3.4804
AlAs	zinc blende	5.6533	83.5/120.4	3760	5.20	2.9383
Al_2O_3	hexagonal	4.785 (a)	345	3980	5.50 ($\perp$)	1.755

Outline

- Brownian noise and crystalline multilayer motivation
  - applications, crystal growth, and basic properties
- Confirmation of high reflectivity and low loss angles
  - damping and thermal noise in micro- and meso-scale mirrors
- Crystalline mirrors for precision measurement
  - bonded “macroscopic” mirrors for optical reference cavities
- Path towards low-thermal-noise LIGO-scale mirrors
  - exploit existing infrastructure for IC fabrication

High-Performance Resonators

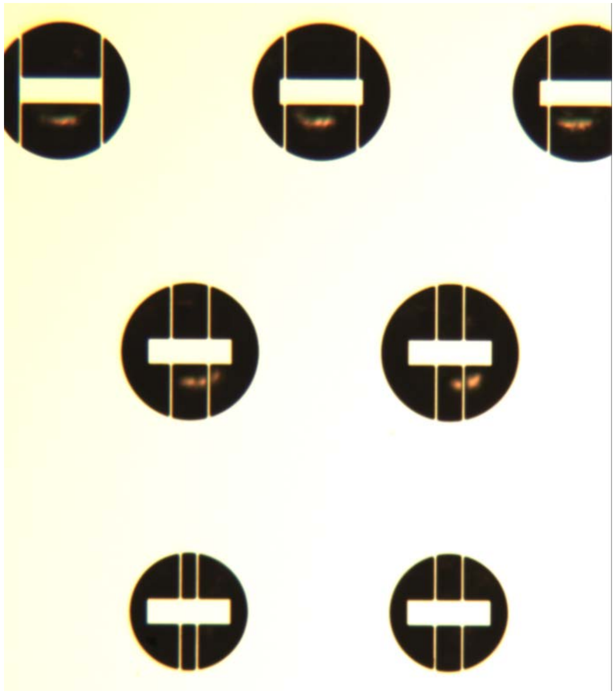

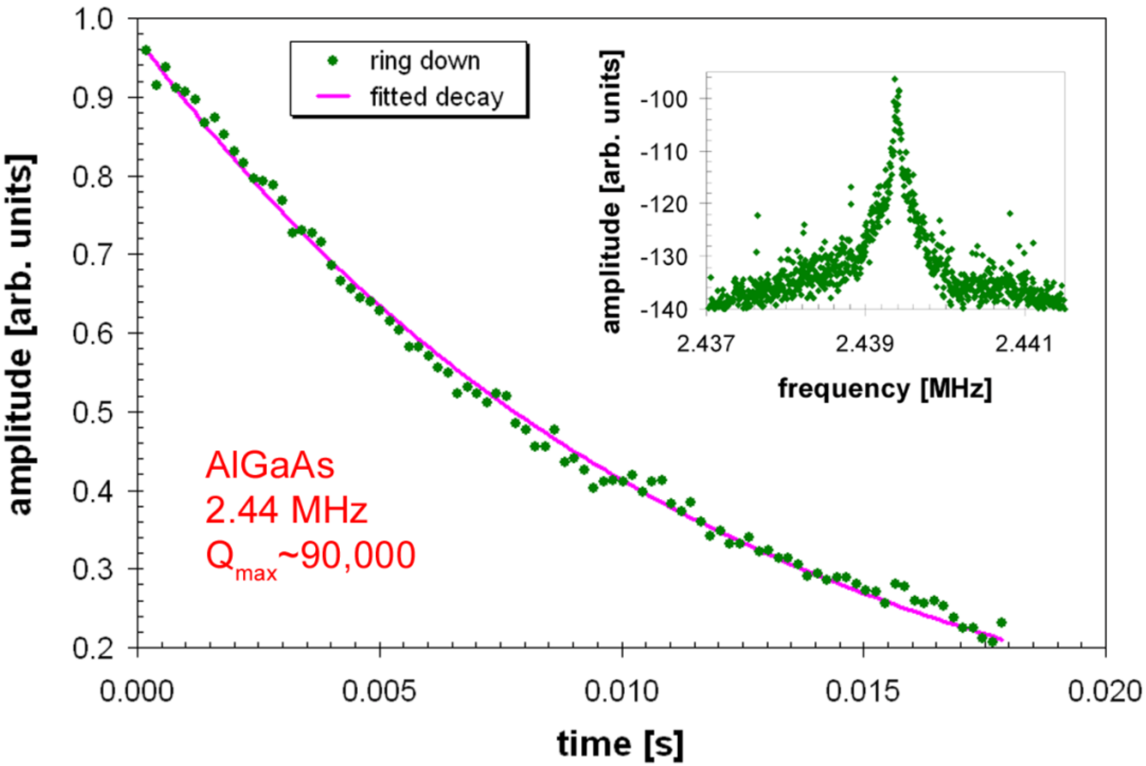

- Highest measured quality factors exceed 1.0×10^5 at ~20 K
- Damping appears to be frequency independent (constant loss angle)
- Maximum finesse of ~20k (limited by scatter and absorption)

G. D. Cole et al., Nature Communications (2011) | G. D. Cole, et al., IEEE MEMS conf. (2010)

Low Frequency Cantilevers

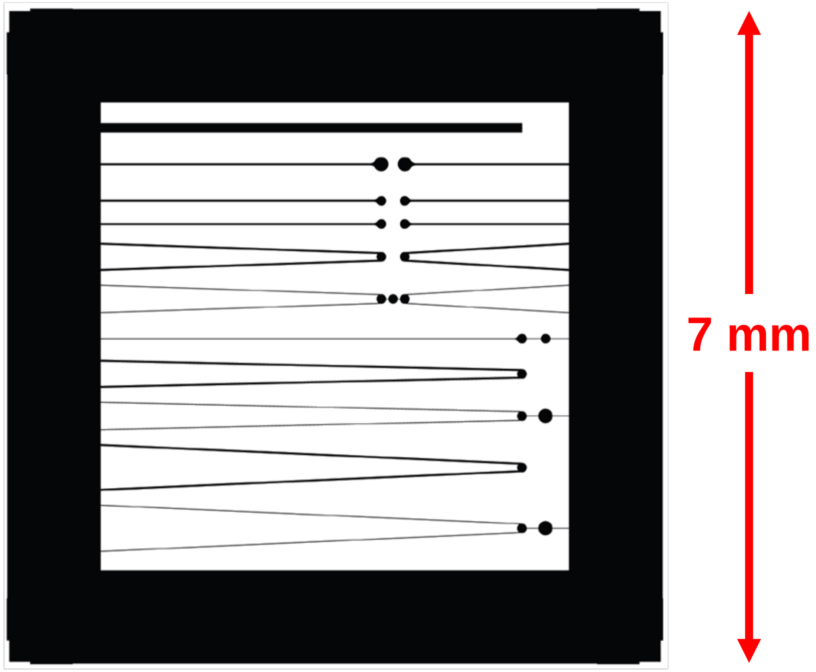

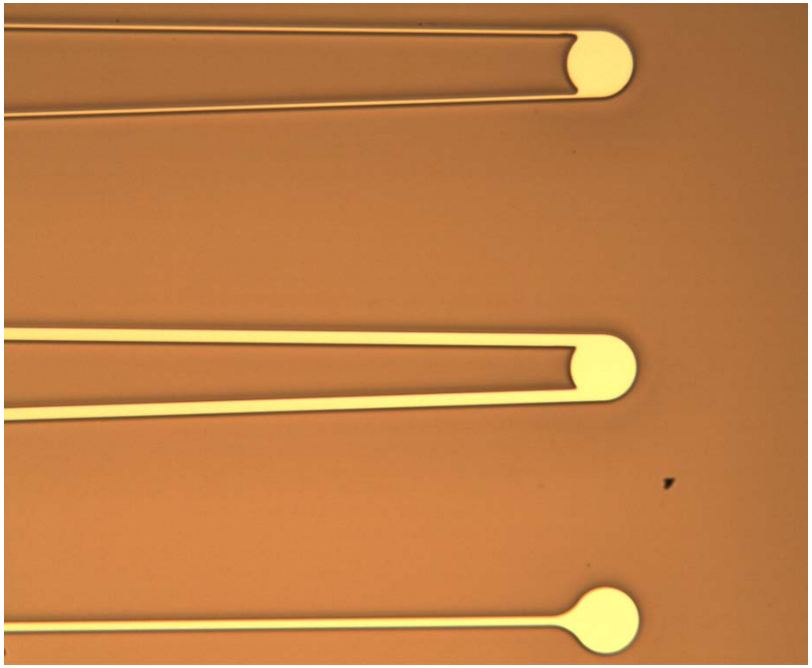

- Monocrystalline mirror sculpted into suspended mm-scale cantilevers
  - aspect ratio (length:min. lateral dimension) = ~1000:1, quite fragile!
- Very low fundamental-mode frequencies and small effective masses
  - 4.5 mm x 6.1 μm x 6.88 μm → 164 Hz (lateral), 184 Hz (out-of-plane)
  - modal mass (out-of-plane with respect to cavity): 500 ng

Ultra-Low Cryogenic Loss Angle

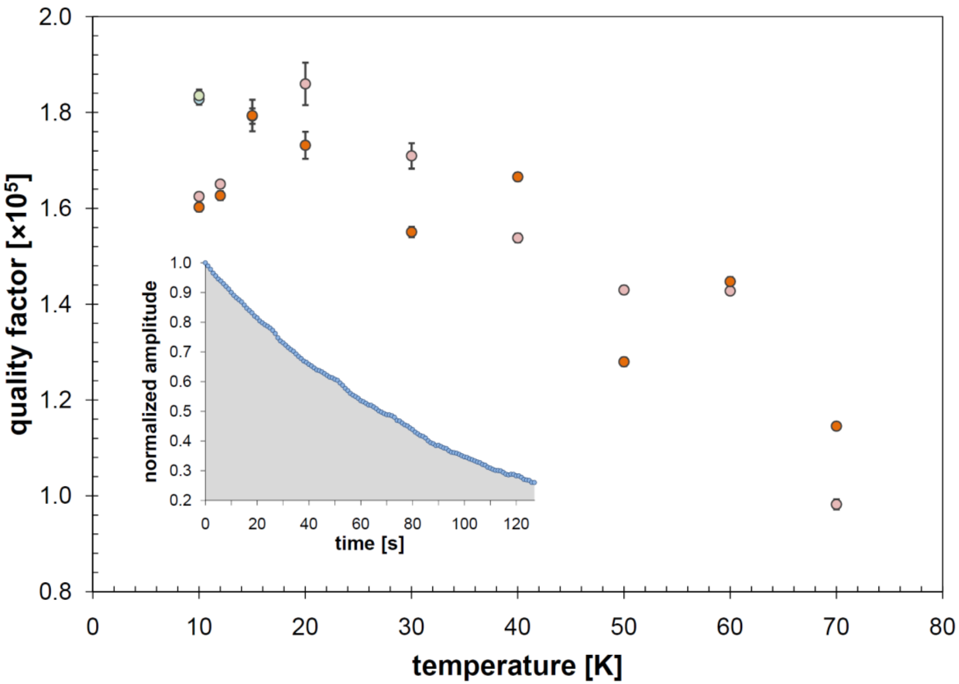

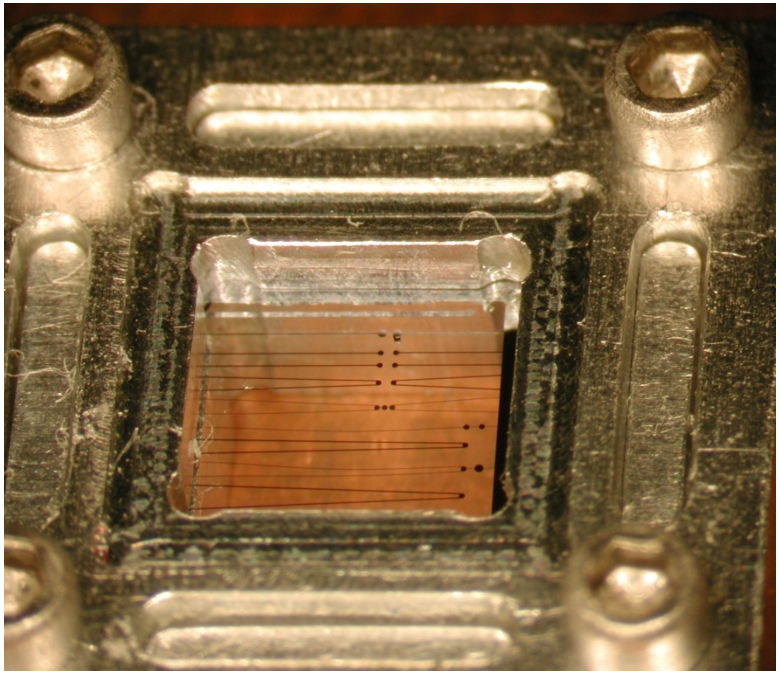

- Finesse up to 30k measured on the suspended cantilever (100 µm pad)
  - reflectivity ultimately limited by scatter and absorption losses
- Ringdown yields Q values 30-40k at RT and exceeding 2×10^5 at 10 K
  - loss angle φ of 4.5×10^{-6}, two orders of magnitude below dielectric mirrors
  - ringdown ~10 minutes (τ ≈ 400 s), extreme vibration isolation required

Room Temp. Thermal Noise

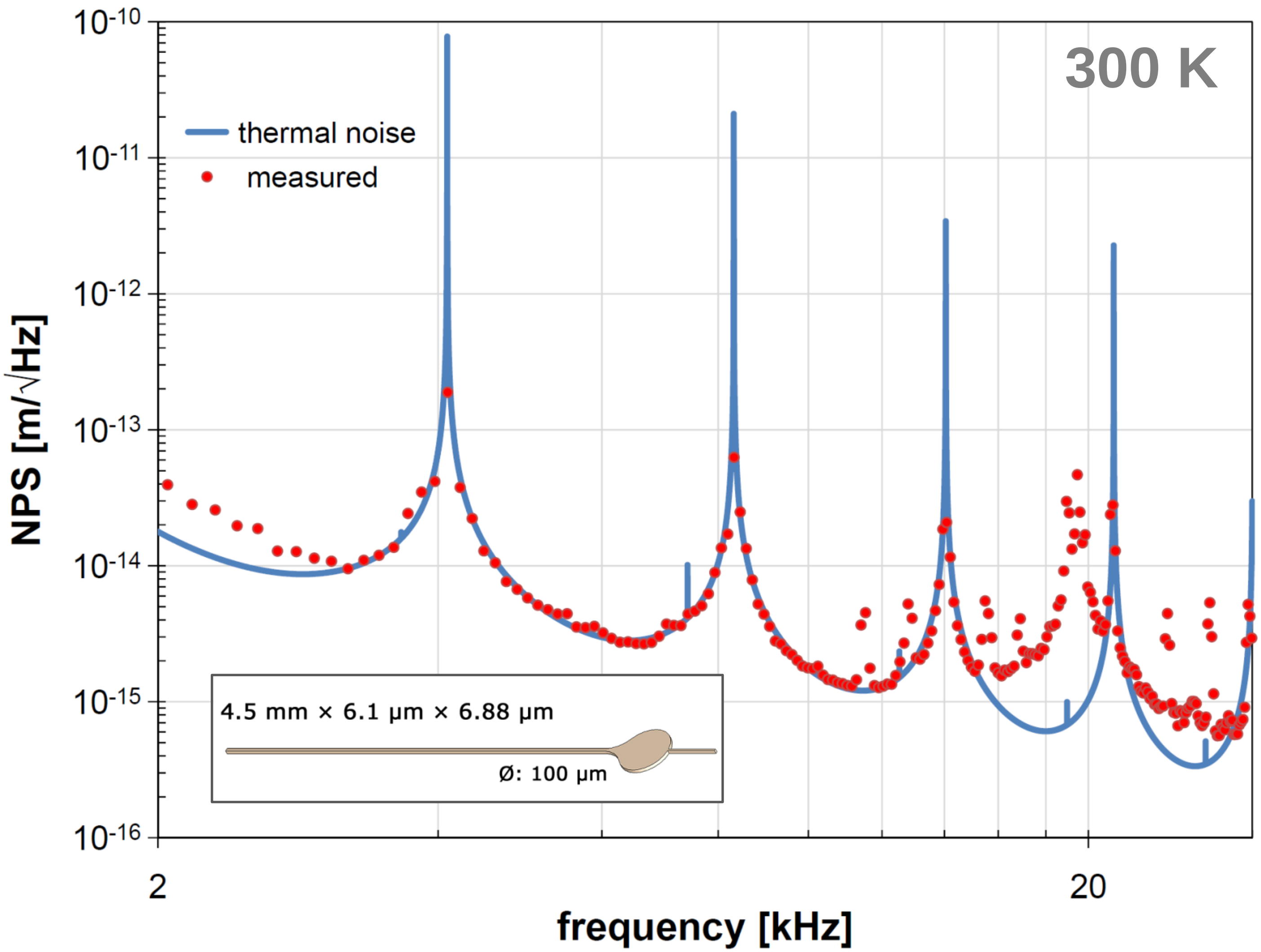

Q: 30k

F: 20k

P_{ext}: 5 μW

S. R. Sankar, G. D. Cole, T. Corbitt, M. Aspelmeyer, N. Mavalvala, manuscript in progress (2012)

Cryogenic Thermal Noise

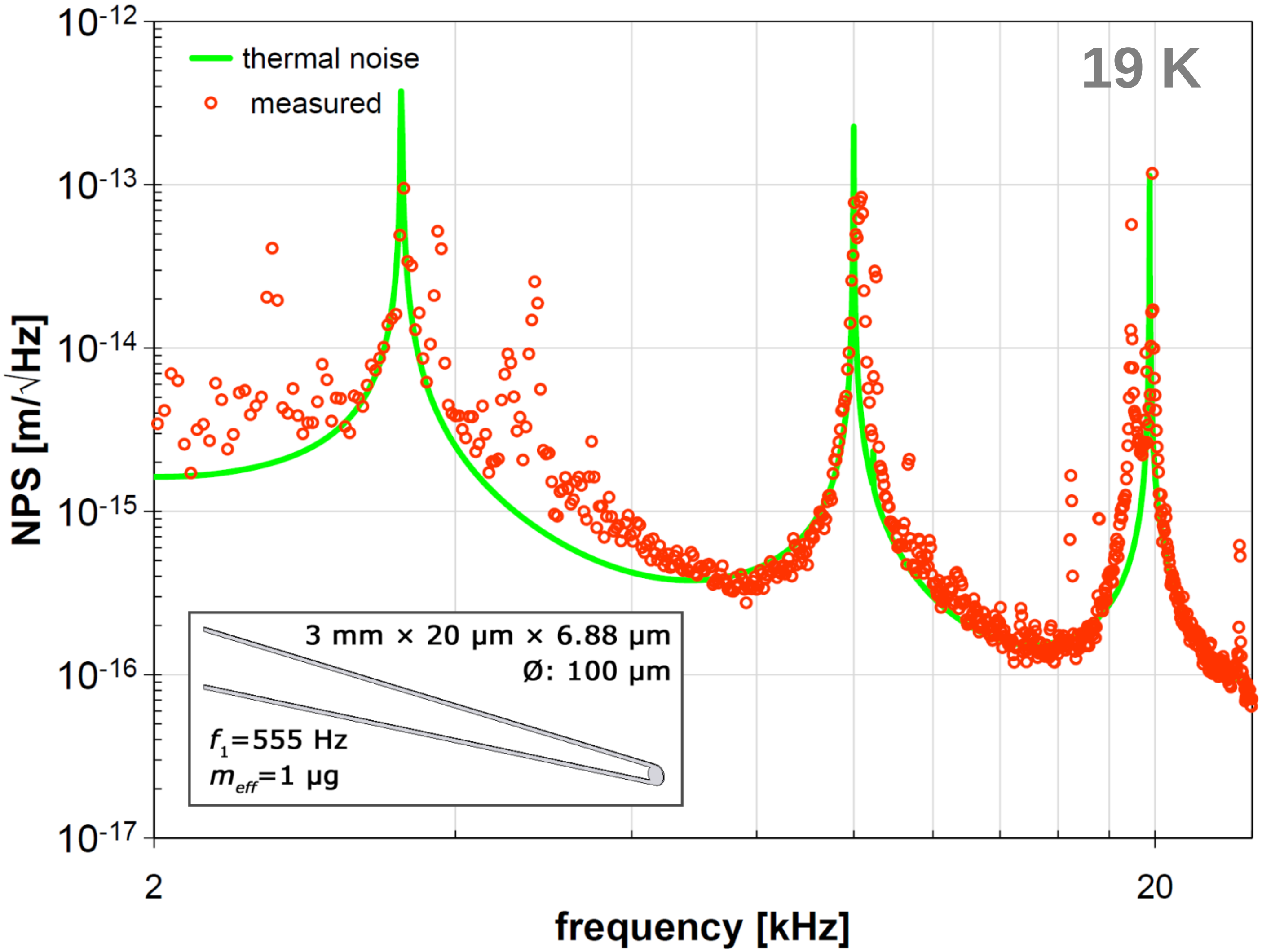

Q: >100k
F: 20k
P_{ext}: 5 μW

S. R. Sankar, G. D. Cole, T. Corbitt, M. Aspelmeyer, N. Mavalvala, manuscript in progress (2012)

Outline

- Brownian noise and crystalline multilayer motivation
  - applications, crystal growth, and basic properties
- Confirmation of high reflectivity and low loss angles
  - damping and thermal noise in micro- and meso-scale mirrors
- Crystalline mirrors for precision measurement
  - bonded “macroscopic” mirrors for optical reference cavities
- Path towards low-thermal-noise LIGO-scale mirrors
  - exploit existing infrastructure for IC fabrication

Ion Beam Sputtered Dielectric Films

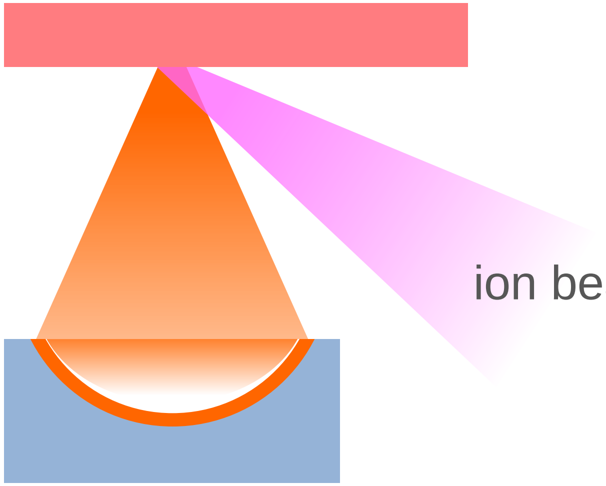

State-of-the-art mirrors
alternating dielectric films, typically SiO_2/Ta_2O_5

Allows for deposition onto essentially arbitrary substrates

- Multilayer of sputtered amorphous films generated via IBS
- Phenomenal optical properties (high R, low absorption and scatter)
- Flexible choice of substrates (assuming proper surface properties)
  - super-polished SiO_2, Si, ULE, sapphire, etc.

Bonded Monocrystalline Mirrors

Minimizing coating thermal noise

Macroscopic mirrors from epitaxial AlGaAs alloys

Direct deposition onto arbitrary substrates precluded by lattice matching condition

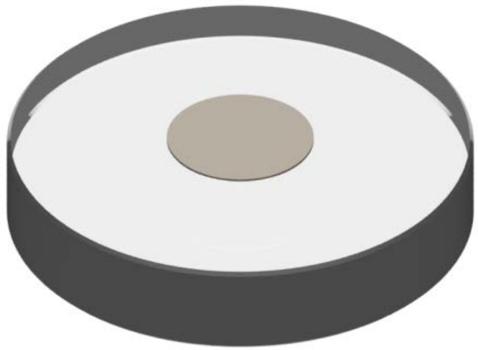

- Employ semiconductor microfabrication techniques to transfer AlGaAs multilayers onto arbitrary substrates (SiO_2, sapphire, etc.)
  - ideal process allows for used of curved mirror blanks
  - identical form factor, no change in overall system design

Transferred Mirror Development

Top view: patterned mirrors on a crystalline substrate

Side view: bonding

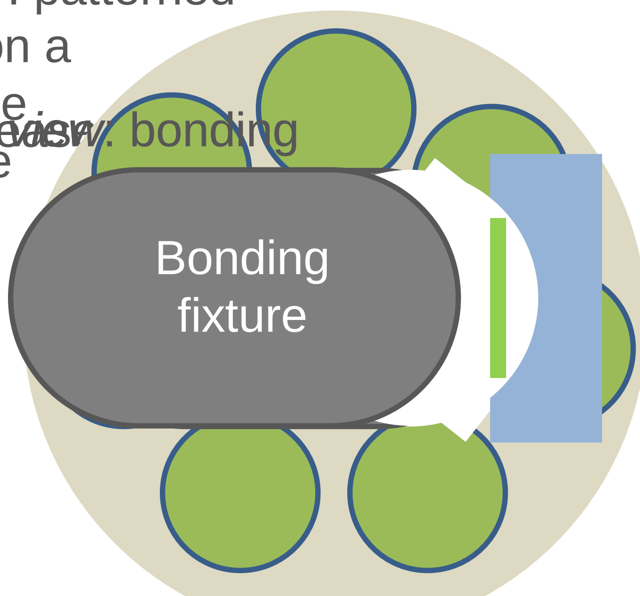

- Free-standing mirror discs transferred onto arbitrary substrates
  - cleanliness and proper handling is crucial for high-yield
  - interfacial energy must be optimized for intended application

Preliminary Cavity Results

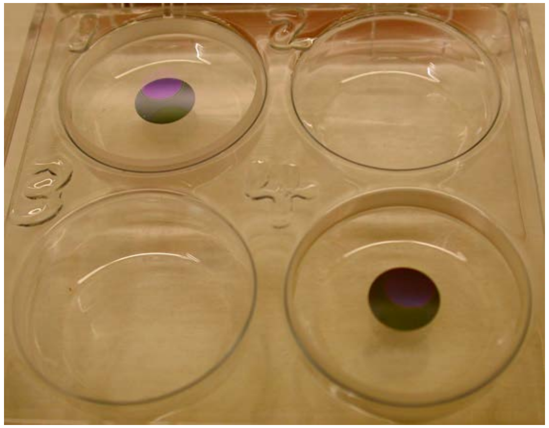

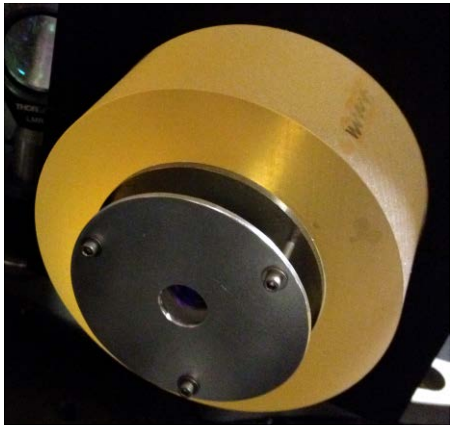

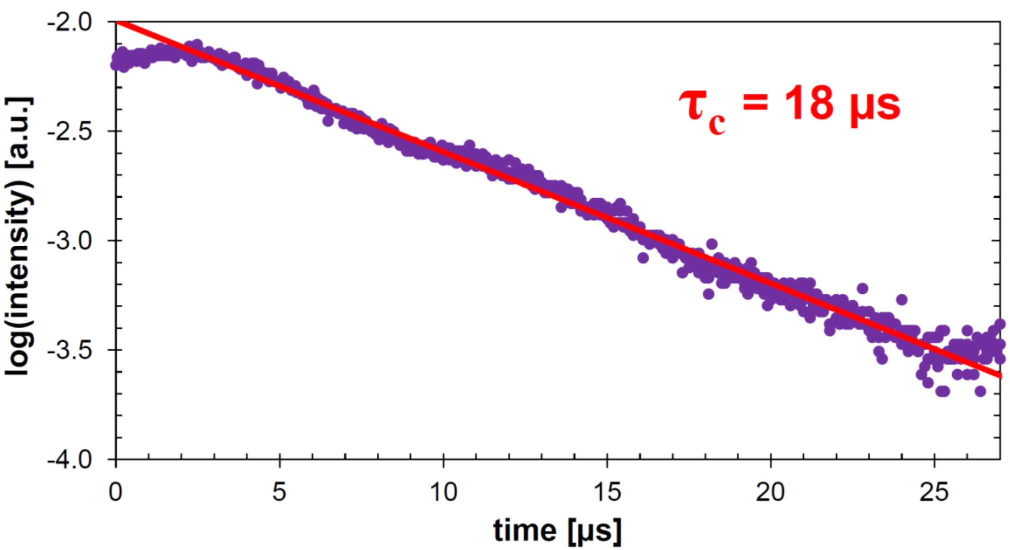

- Hybrid cavity at JILA
  - ULE spacer with clamped AR-coated end mirrors
  - planar and 1-m ROC fused-silica substrates
  - Length = 24 cm
- Initial finesse of 0.75×10^5
  - theory ~ 1.4×10^5
  - cleanliness limited?
- Next steps:
  - clean thoroughly
  - contact to fixed spacer
  - double check finesse and measure thermal noise

in collaboration with Mike Martin and Craig Benko from Jun Ye's group at UC Boulder / JILA

Outline

- Brownian noise and crystalline multilayer motivation
  - applications, crystal growth, and basic properties
- Achieving high reflectivity and ultra-low loss angles
  - damping and thermal noise in micro- and meso-scale mirrors
- Crystalline mirrors for precision measurement
  - bonded “macroscopic” mirrors for optical reference cavities
- Path towards low-thermal-noise LIGO-scale mirrors
  - exploit existing infrastructure for IC fabrication

Towards LIGO-scale Mirrors

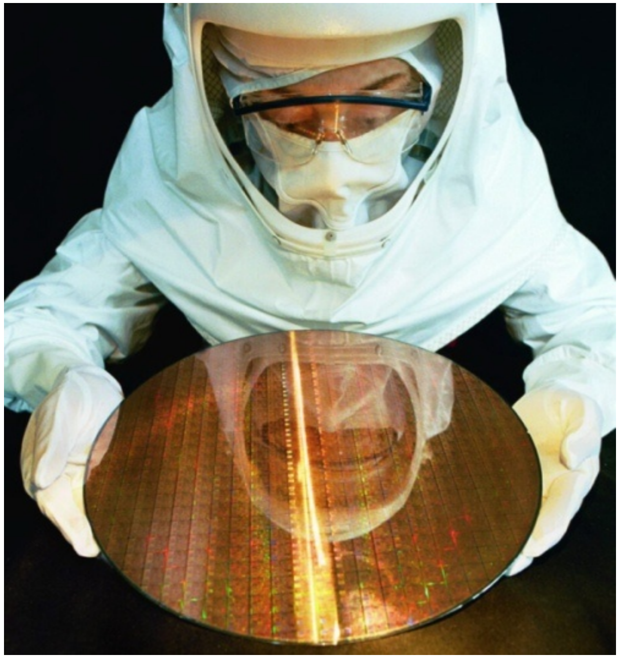

- Leverage infrastructure for semiconductor fabrication
  - high-uniformity epitaxial growth on large-diameter substrates
  - void-free direct bonding of crystalline semiconductors

Towards LIGO-scale Mirrors

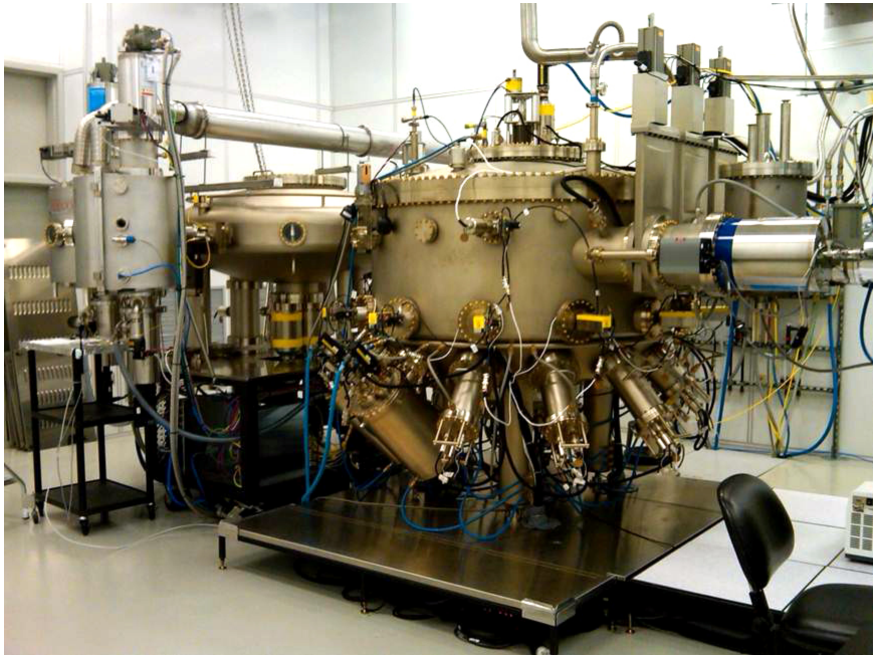

- Production MBE reactors for microwave electronics
  - 7 x 150-mm or 4 x 200-mm wafers (Veeco GEN2k/Riber R7k)
- Direct bonding systems for SOI wafer production
  - industrial tools capable of bonding 450-mm diam. wafers

* Photo credit: Bob Yanka, RFMD; Veeco GEN2000 multi-wafer production MBE system

Summary of AlGaAs Mirror Properties

- Substrate-transferred crystalline mirrors are a promising avenue for future gravitational wave detectors
- More than **100×** decrease in mechanical loss angle
  - cryogenic Q-values $>1\times10^5$ ($\varphi_{min}=4.5\times10^{-6}$) at 180 Hz-4 MHz
  - room temperature Q-values $\sim4\times10^4$ ($\varphi_{min}=2.5\times10^{-5}$)
  - compares with typical φ of $\sim3\times10^{-4}$ for SiO_2/Ta_2O_5
- Potential for very low scatter loss and absorption
  - MBE-grown films: 1-2 Å RMS surface roughness
  - ~10 ppm ($\alpha=0.2$ cm^{-1}) absorption at 1064 nm (2 W, 70 μm Ø)
- Reflectivity >99.99% measured for 40.5 layer pairs
  - potential for finesse $\sim10^5$ (preliminary results from JILA)

Blatant Self-Promotion

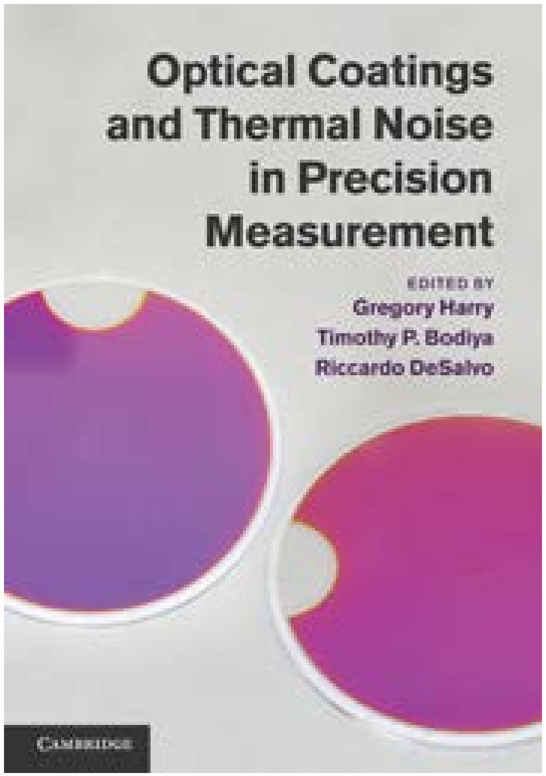

CAMBRIDGE
UNIVERSITY PRESS

Available now at Amazon.com ☺

<u>Editors</u>:
Gregory Harry
American University, Washington DC

Timothy P. Bodiya
Massachusetts Institute of Technology

Riccardo DeSalvo
Università degli Studi del Sannio, Italy

Chapter 16, “Cavity Optomechanics,” by G. D. Cole and M. Aspelmeyer contains the compiled results of our work on AlGaAs-based epitaxial Bragg mirrors

Macroscopic DBR Development

- Direct bonding of GaAs to silicon and SiO_2 has been demonstrated for wafers with diameters up to 150 mm
  - direct and LT oxide/oxide bonding
  - limited to *flat* structures

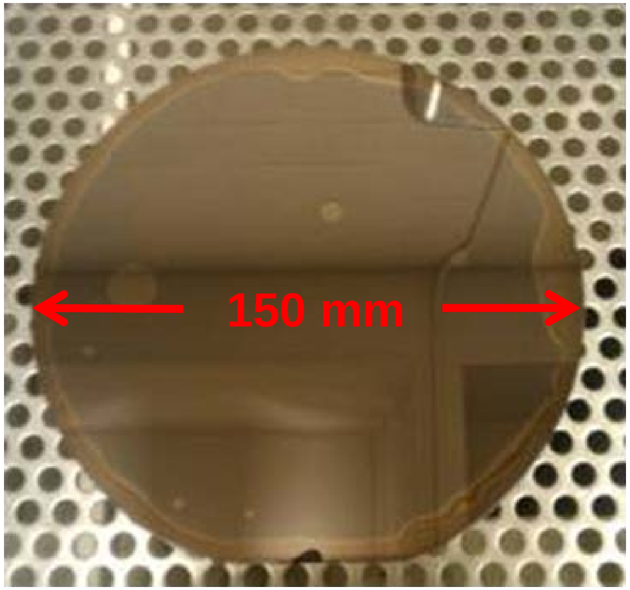

- Reference cavity relevant bonding
  - 25-mm Ø fused silica mirror blanks
  - planar and curved mirrors required
- Enemies: voids and inclusions
  - will research lab environment be sufficient for prototyping?
  - optimized cleaning and handling procedure is key to success!

Y. Bai, G. D. Cole, M. T. Bulsara, E. A. Fitzgerald, Journal of the Electrochemical Society (2012)

Open Questions

1) What are the ultimate limits of Q for these materials?
2) Are we approaching the minimum absorption level?
3) Can we minimize for thermo-optic effects at RT?
4) Is damping of bonded interface a potential roadblock?
5) What is the minimum achievable radius of curvature?

Alternative Reflector Technologies

- Resonant waveguide grating-based reflectors (Jena)
  - polycrystalline-Si/SiO_2 'double T' grating structure
  - R_{theory} ~99.95%, first iteration R=89%, limited bandwidth
- Epitaxial films on crystalline Si substrates (Stanford)
  - possibility of realizing crystalline AlGaP/Si multilayers
  - initial work on MBE grown films pioneered in mid '80s

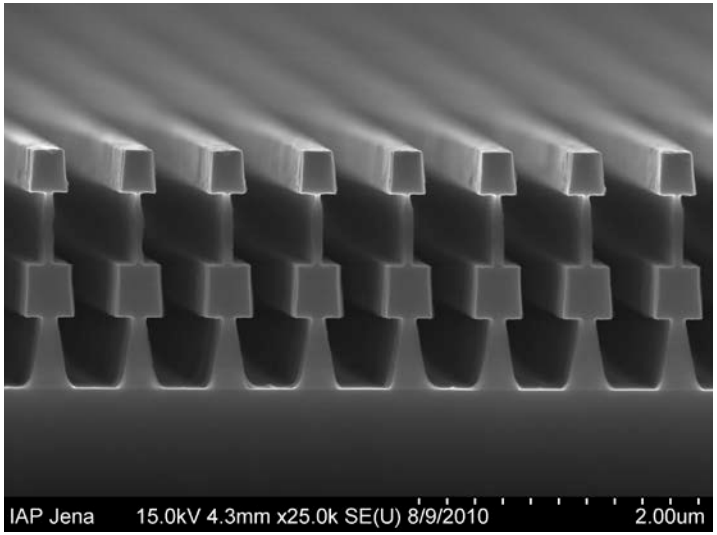

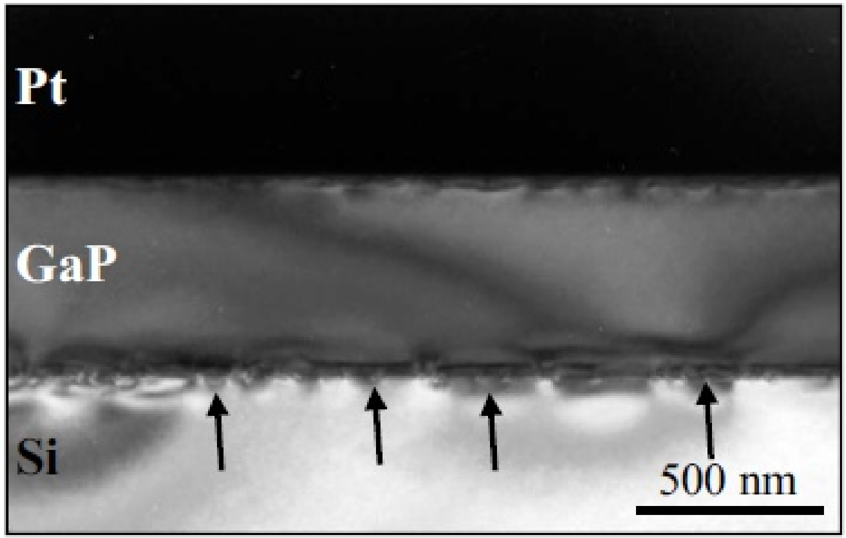

S. Kroker, et al., Optics Express 19 (2011) | T. J. Grassman, et al., Appl. Phys. Lett. 94 (2009)

Measurement of Bonded Prototype

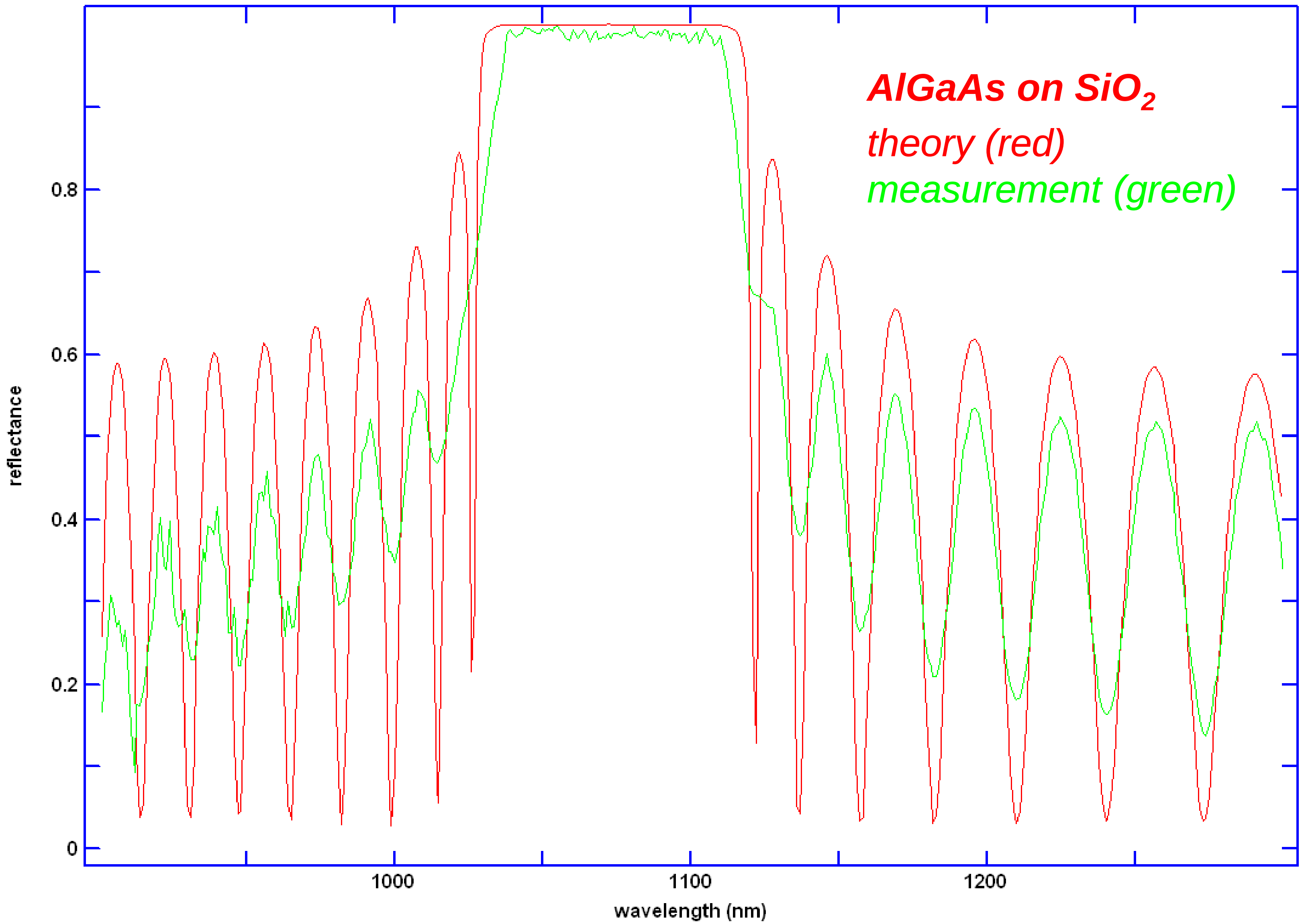

Epitaxial Multilayer Applications

- Epitaxial DBRs originally developed for VCSELs
  - demonstrated in 1983 by K. Iga's group at the Tokyo Institute of Technology
  - VCSEL consists of high-reflectivity mirrors surrounding a semiconductor microcavity
  - circularly symmetric emission normal to the substrate surface (very efficient fiber coupling)
- Lattice matching constraint limits substrate choices
  - AlInGaAs:GaAs, InGaAsP:InP

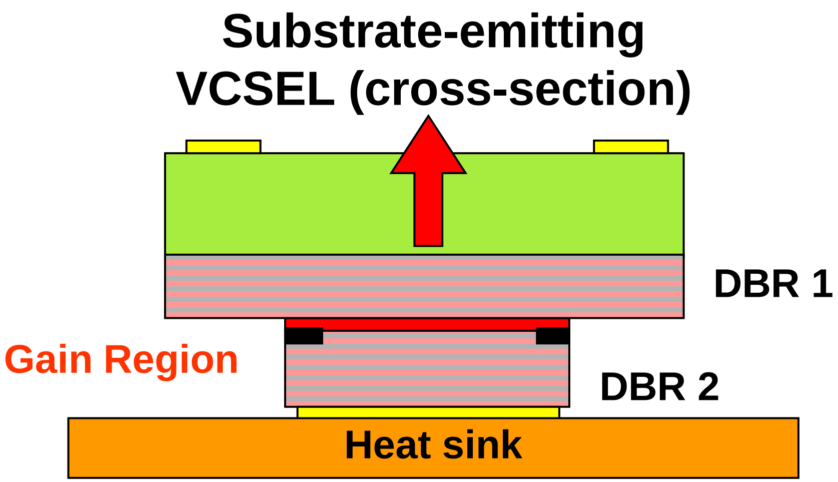

III-V "Map of the World"

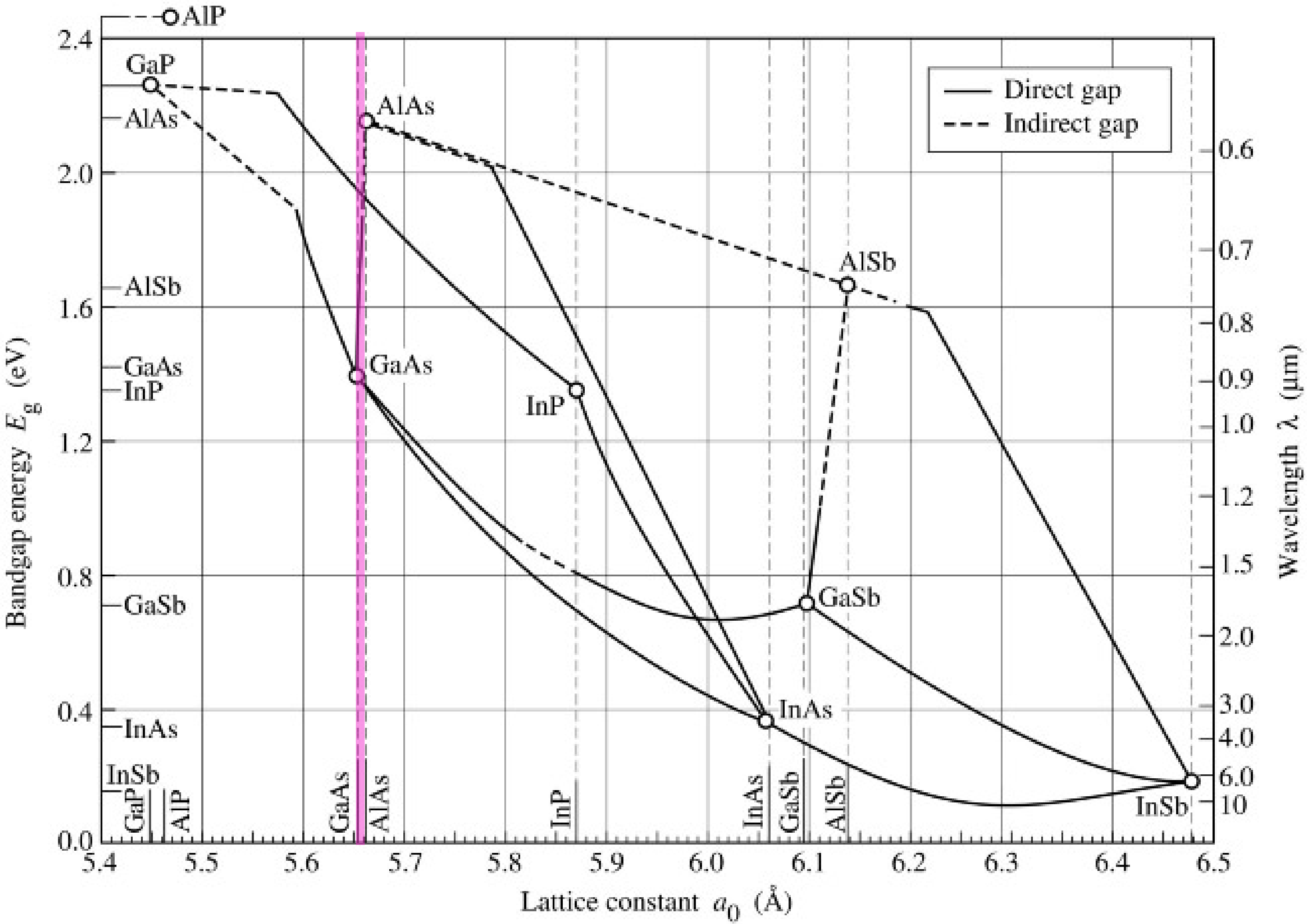

Radiation Pressure Shot Noise

- Noise experienced by a suspended body due to photon number fluctuations in incident laser beam
  - quantum back-action of optical displacement measurement
  - ideal system would simultaneously achieve low frequency and low mass (nanogram and sub-kHz in same structure)

$$\delta_{x_{rad}} = \frac{2F}{m_{eff}\,\omega^2}\sqrt{\frac{\hbar P_{ext}}{\pi \lambda c}}$$

↑ *reflectivity and Q*

units: m/√Hz

↓ *frequency & mass*

Thermal noise of mechanical system is a major obstacle for observing this effect, solution: *low-loss crystalline mirrors*

Thermal Noise Theory

$$\delta_{x_t} = \left[\sum_{n=1}^{\infty} \frac{4 k_B T \phi \, \omega_n^2}{m_{eff,n} \, \omega \left[\left(\omega_n^2 - \omega^2 \right)^2 + \left(\phi \, \omega_n^2 \right)^2 \right]} \right]^{\frac{1}{2}}$$

units: m/√Hz

- Thermal noise spectrum: sum of noise of all modes
  - requires eigenfrequency, effective mass, and loss angle

- Eigenfrequencies and effective masses via FEM
  - elastic constants of AlGaAs single-crystal (proper orientation)
  - as-fabricated geometry (measured modes as guidelines)
  - Gaussian “probe” for optically-sampled effective mass
  - measured Q value for obtaining proper loss angle

P. R. Saulson, Phys. Rev. D 42, 2437 (1990)

Predicted Cryogenic Results

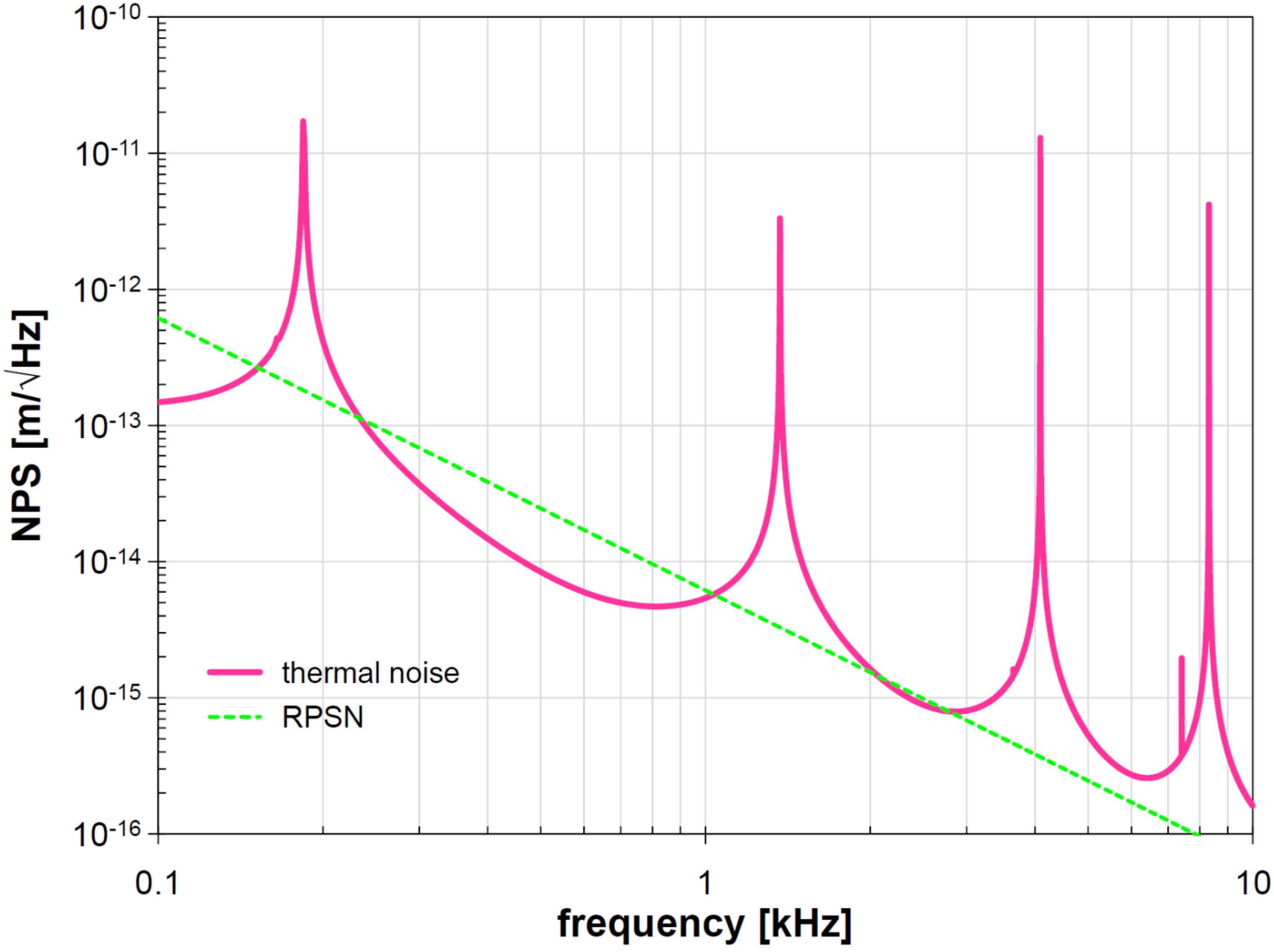

Q: 120k
F: 20k
P_{ext}: 10 μW

Experimental Details

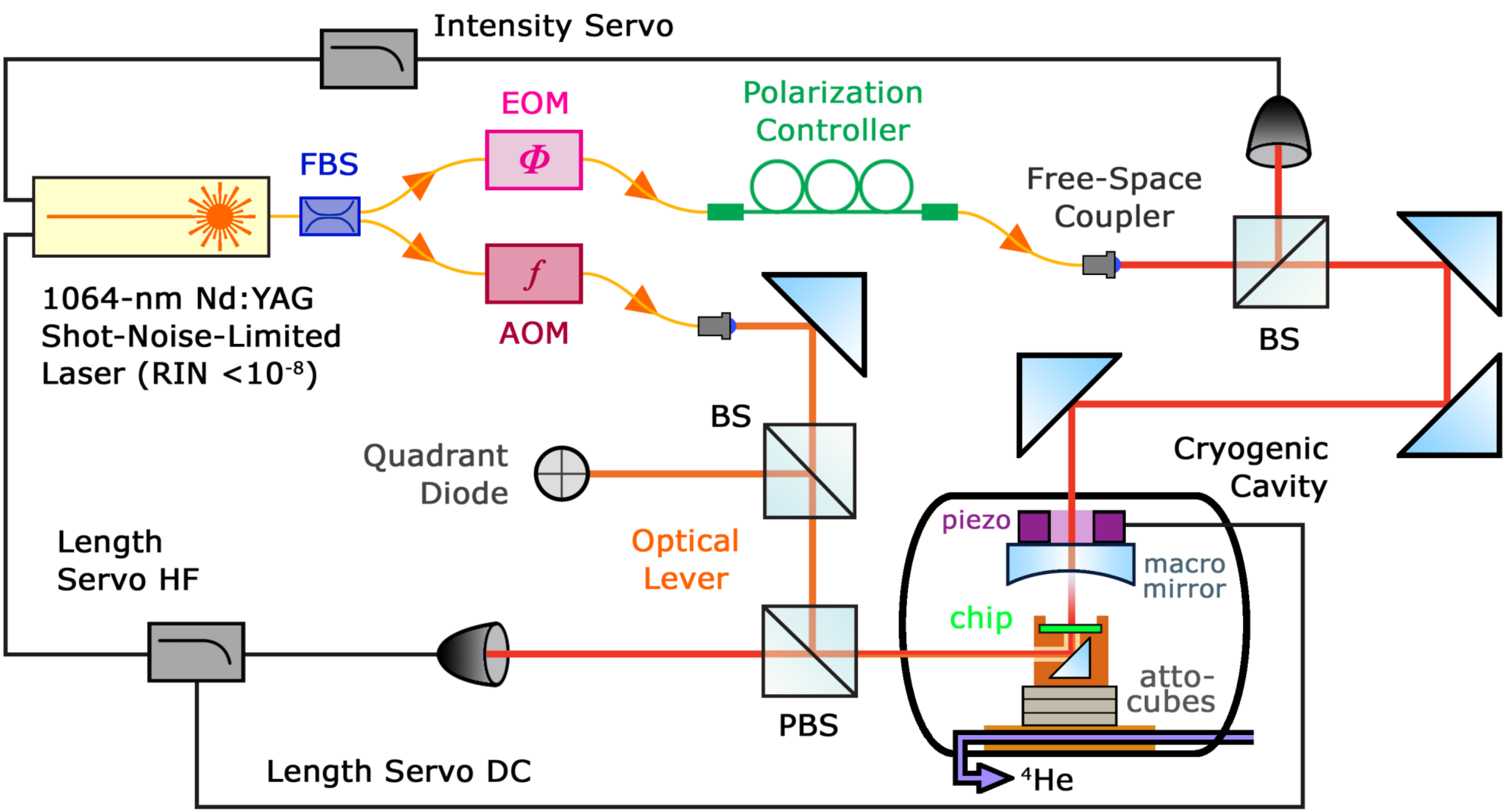

Monocrystalline Optomechanics

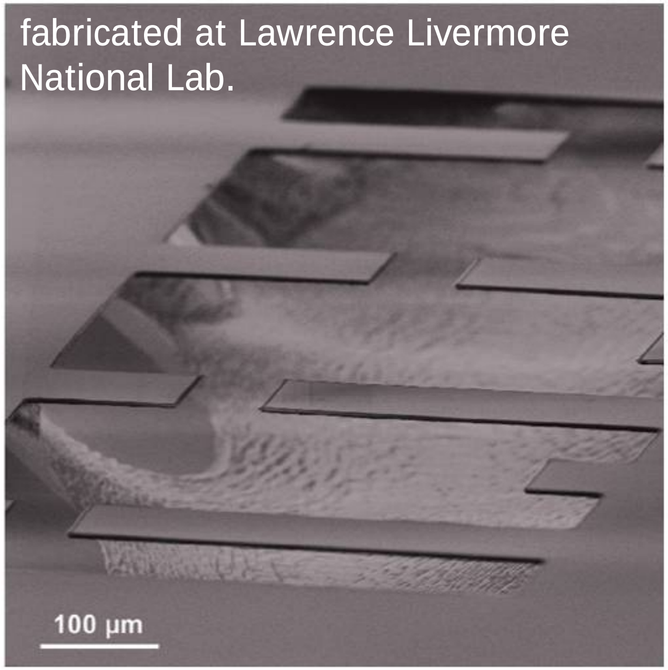

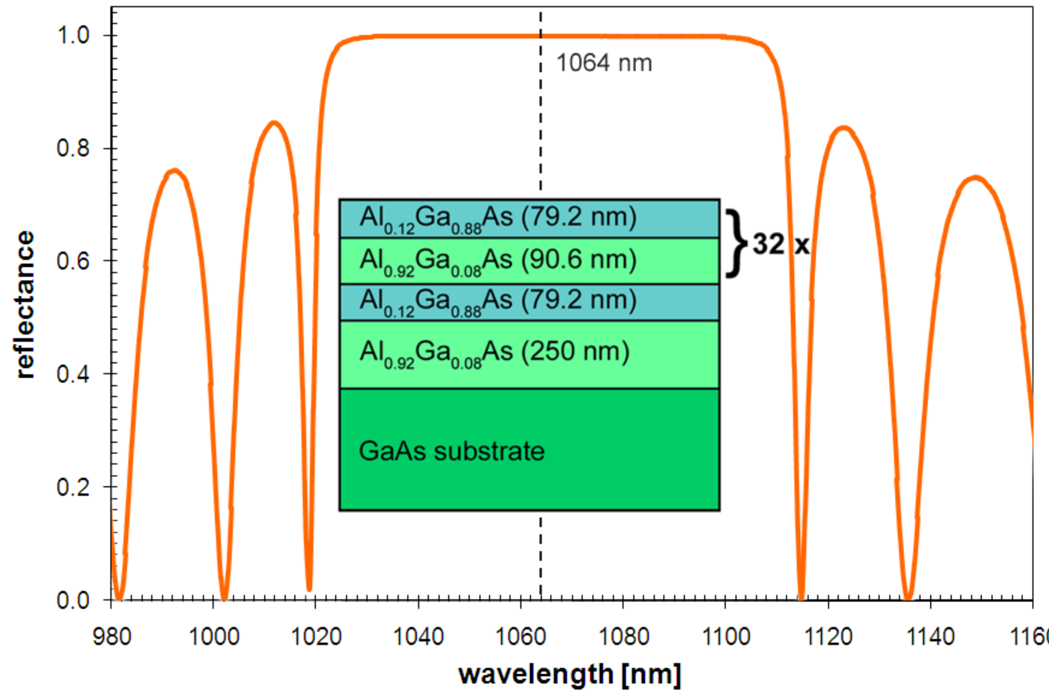

- 32.5 period undoped $Al_xGa_{1-x}As$ distributed Bragg reflector (MBE)
  - high index layers contain 12% Al for substrate etch selectivity
  - 8% Ga incorporated in low index film to slow oxidation in ambient
- Single- and doubly-clamped beams, dimensions: 100s x 50 x 5.5 μm^3
  - eigenfrequencies up to 2 MHz (sideband resolved operation κ/ω_m~0.2)

G. D. Cole, et al., Appl. Phys. Lett. 92, 261108 (2008)

AlGaAs Micromirror Process Flow

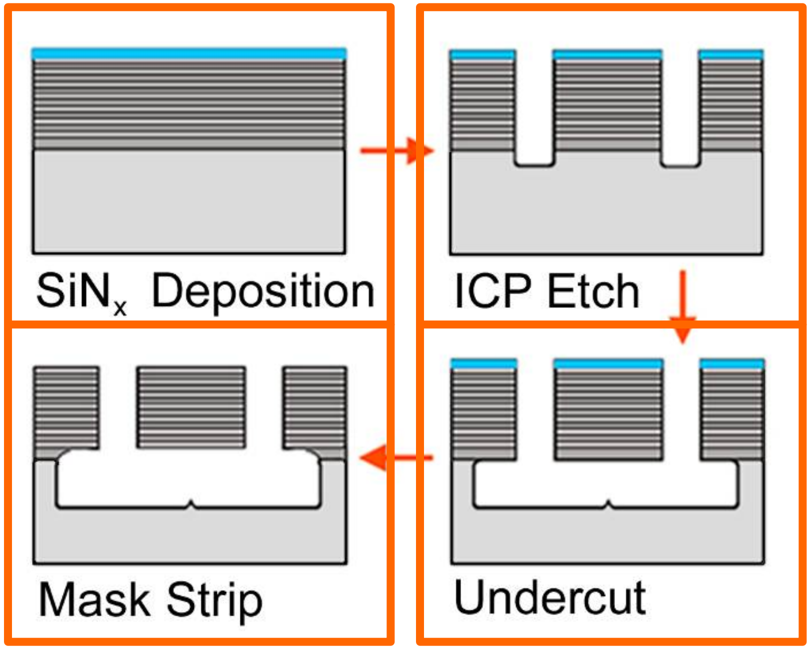

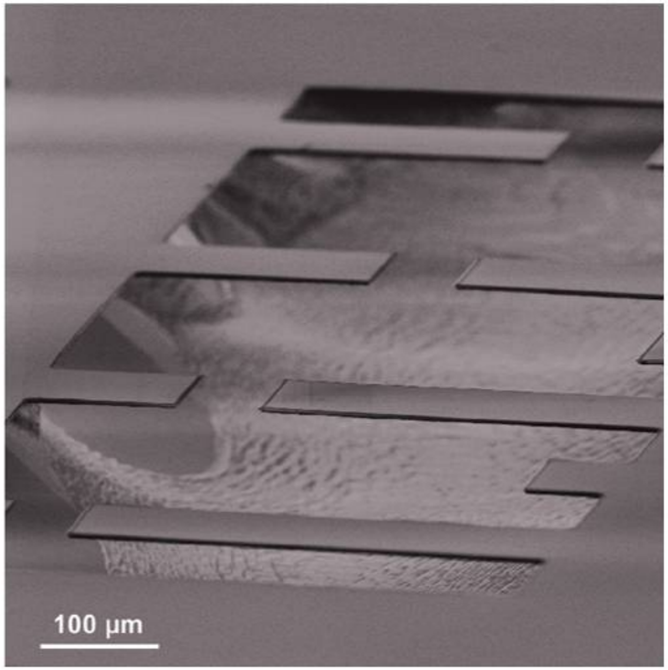

1. Mirror surface protection: PECVD SiN_x (300 ° C, 100-nm thickness)
2. Define mechanics: $SiCl_4/N_2$ ion etch through DBR and into substrate
3. Undercut: selective GaAs wet etch with buffered citric acid solution
4. Strip mirror protection: dilute HF for SiN_x and $Al_{0.92}Ga_{0.08}As$ removal

Finesse and Surface Roughness

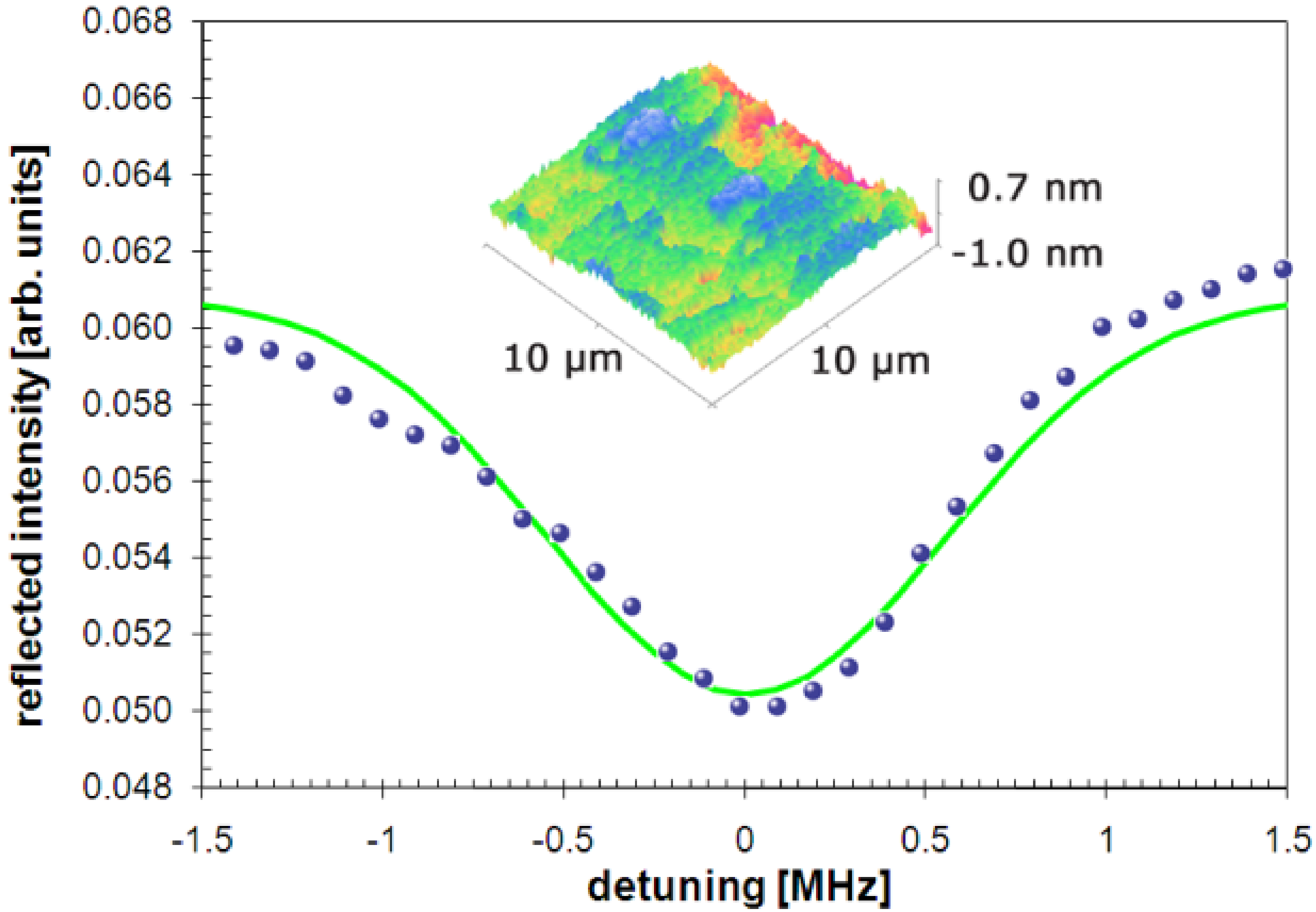

- Atomic force microscopy reveals roughness values below 2 Å
- Material allows for an impedance matched Finesse of 1×10^4

Gen. I Crystalline Mirror Performance

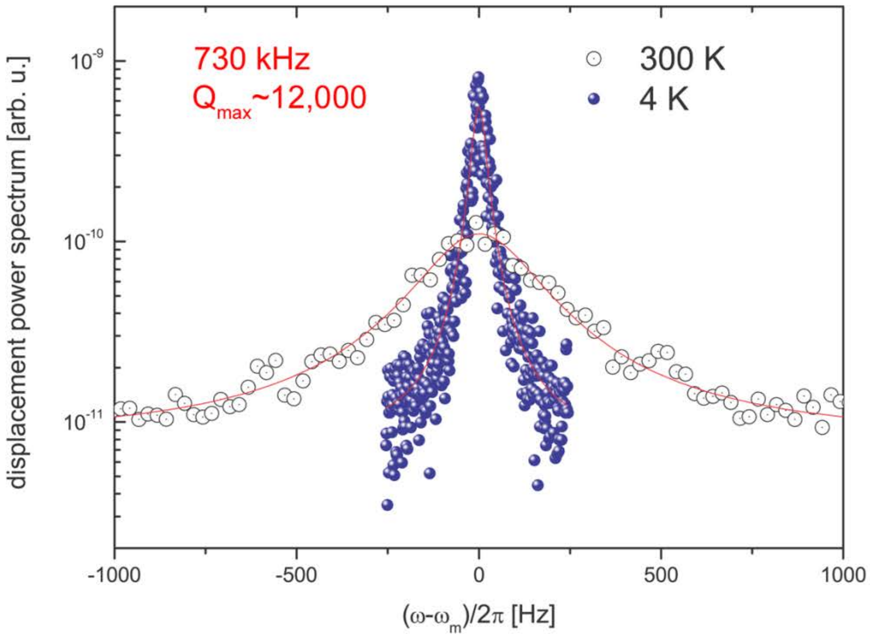

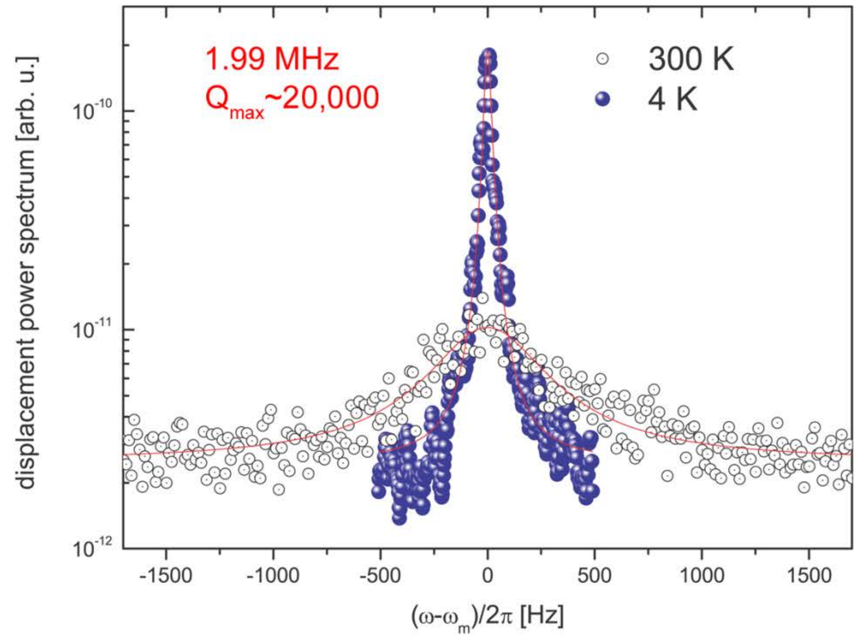

- Mechanical Q shows significant improvement over SiO_2/Ta_2O_5
  - doubly-clamped beams: 2×10^4 versus 0.3×10^4 at 4 K
  - further analysis revealed Q to be anchor-loss limited
- Optical properties are promising: low scatter and absorption loss
  - absorption ~10 ppm, transmission limited R of ~99.98%

Outline

- Motivation for exploring monocrystalline mirrors
  - basic properties, crystal growth, and initial devices
- High-performance “free-free” resonators
  - minimizing mechanical damping through geometric design
- Floppy mirrors: low-frequency microgram cantilevers
  - towards the observation of radiation pressure shot noise
- Crystalline mirrors for precision measurement
  - AlGaAs DBRs for macroscopic cavity end mirrors
- Summary of properties and path forward
  - outlook and discussion of remaining questions

"Phonon-Tunneling" Dissipation

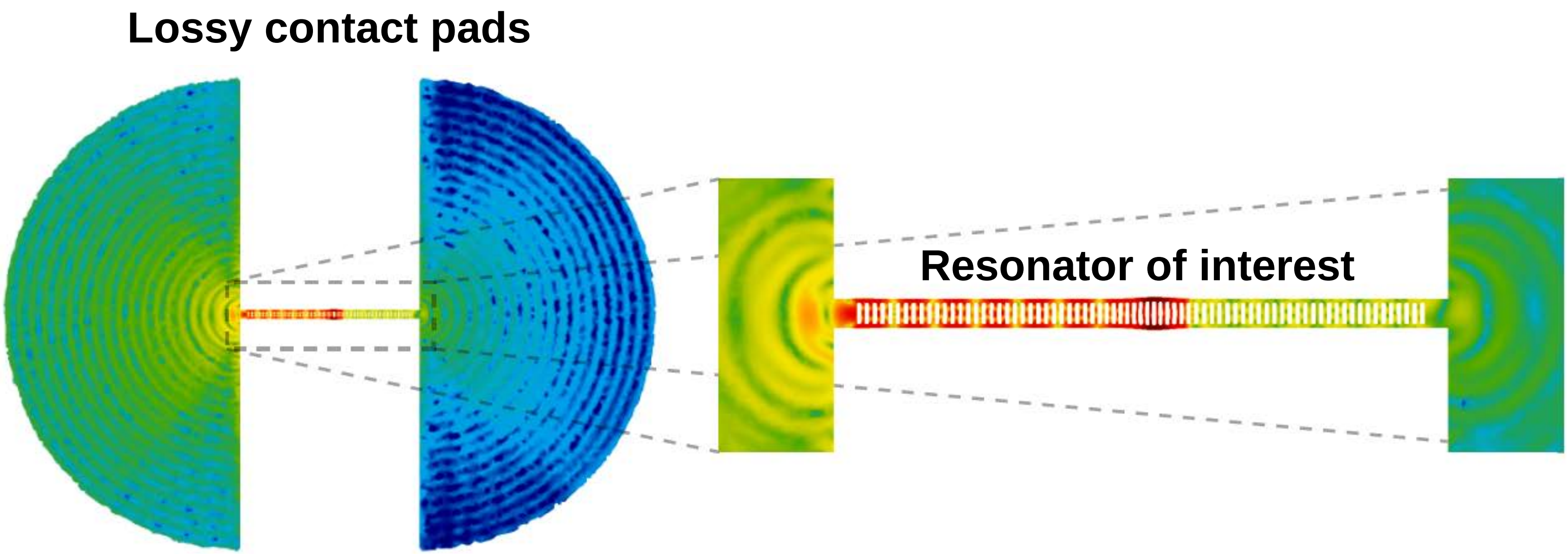

- Fundamental loss mechanism in all suspended resonator structures
  - temperature independent process; intrinsic limitation to quality factor
- Previous approaches to modeling this process are quite cumbersome
  - simulations include large contact area; artifical loss introduced to substrate
  - rigorous solution to elastic wave propagation beyond suspension points

M. Eichenfield, J. Chan, R. M. Camacho, K. J. Vahala, O. Painter, Nature (2009)

Design Dependent Damping

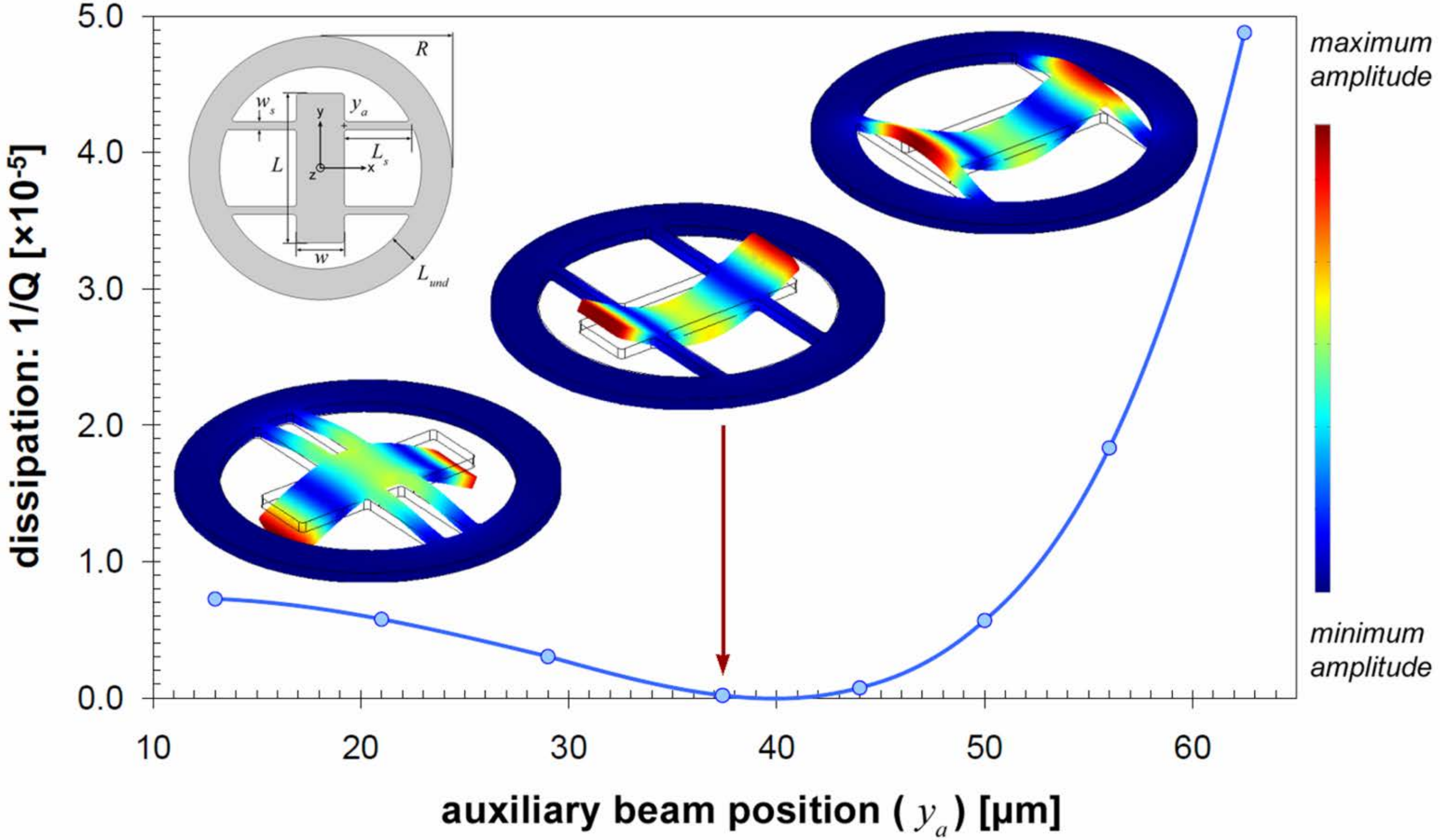

- Ideal resonator design for isolating support-induced losses
- Geometry variation with ~ constant frequency & surface-to-volume ratio

G. D. Cole and I. Wilson-Rae, et al., Nature Communications 2, 231 (2011)

Fabricated Free-Free Resonator

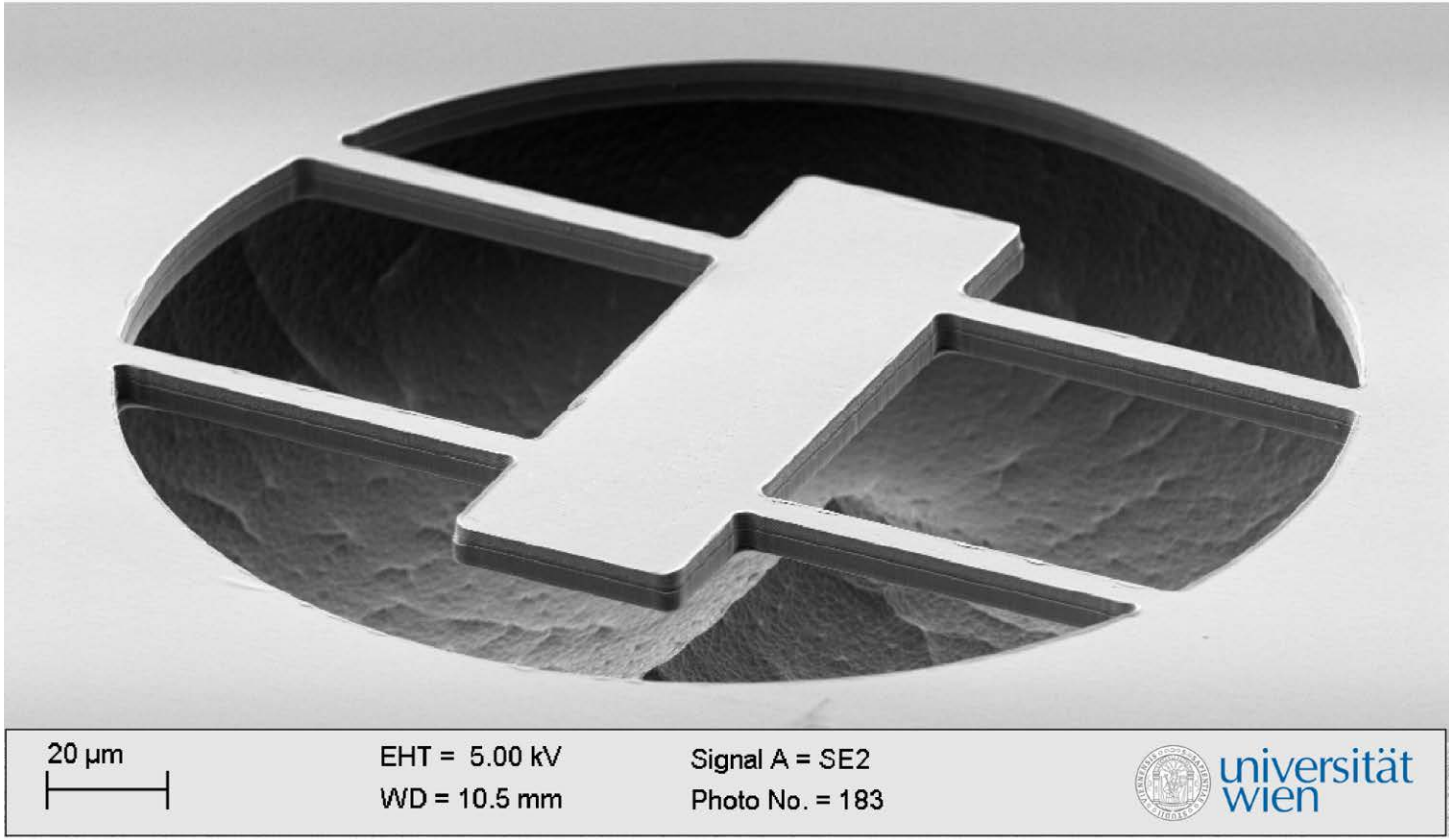

- Single-mask bulk micromachining process, excellent geometric control
- XeF_2 provides near infinite selectivity in Ge etch over GaAs/AlAs DBR

G. D. Cole, Y. Bai, M. Aspelmeyer, and E. A. Fitzgerald, Appl. Phys. Lett. 96, 261102 (2010)

Updated Epitaxial DBR

FBH Leibniz Ferdinand-Braun-Institut

- Identical materials structure as DBR in initial experiments
  - 40 periods rather than 32 to minimize transmission losses
- In-situ growth monitor leads to excellent thickness control
  - target wavelength 1077 nm, measured peak at 1079 nm
  - thickness deviation of ~8 nm over 7.1 µm (0.11 % error!)
- Measured reflectivity >99.99%
  - matched finesse of 1.75×10^4

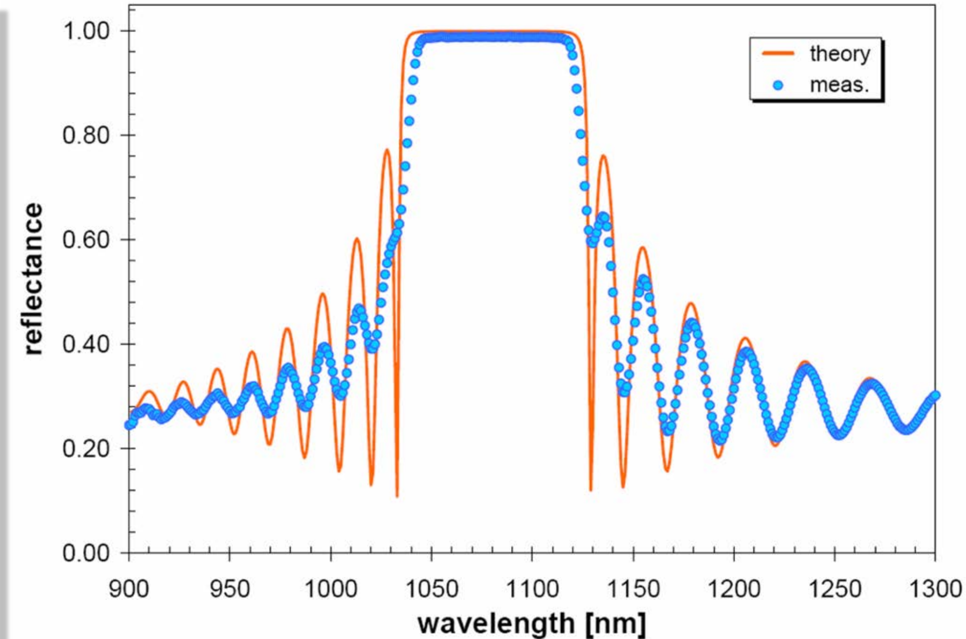

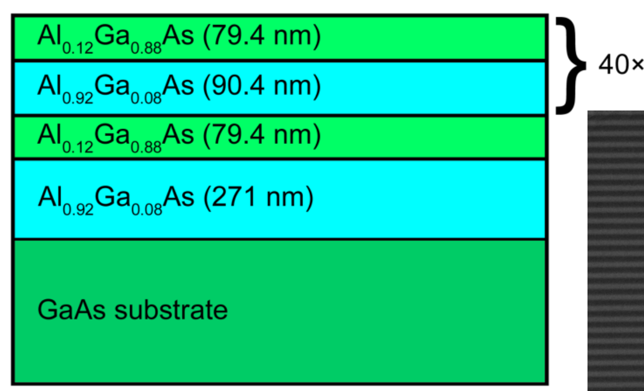

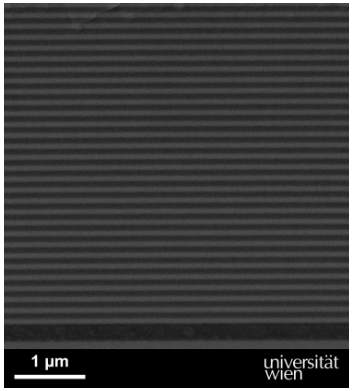

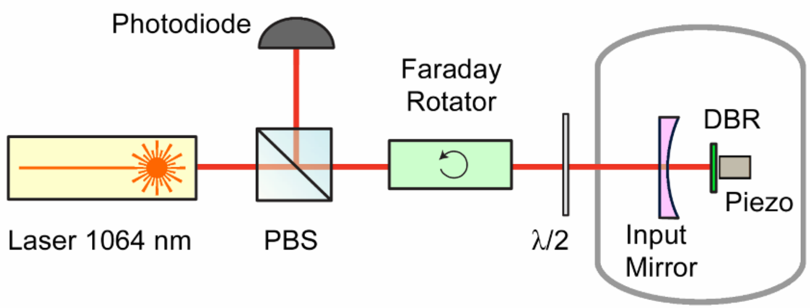

Minimizing the Bath Temperature

- Closed cycle dilution fridge with double-sided optical access
- Base temperature ~25 mK (no input laser), experiments @ 100 mK
- Stable operation of optomechanical cavity recently realized (F >10,000)

$$k_B T/\hbar Q \ll \kappa \ll \omega_m, g_0\alpha$$

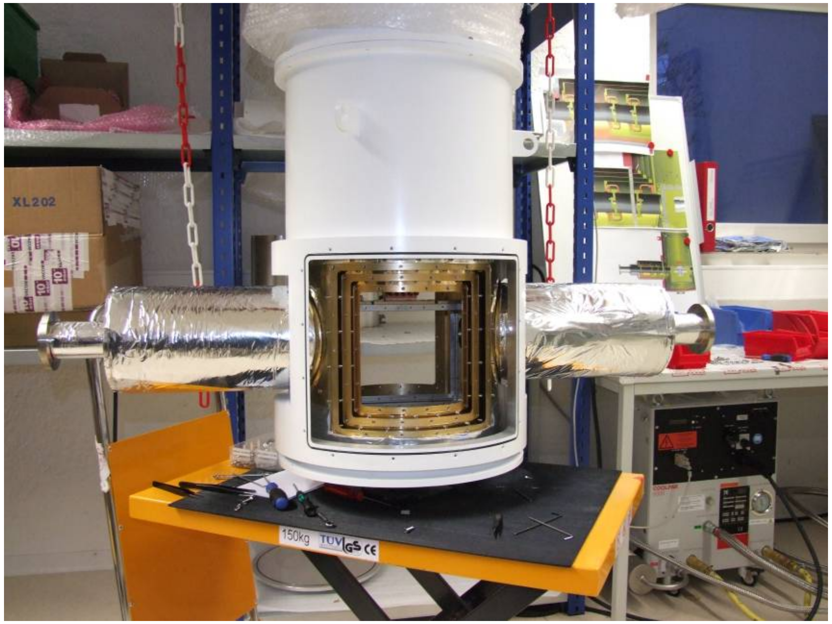

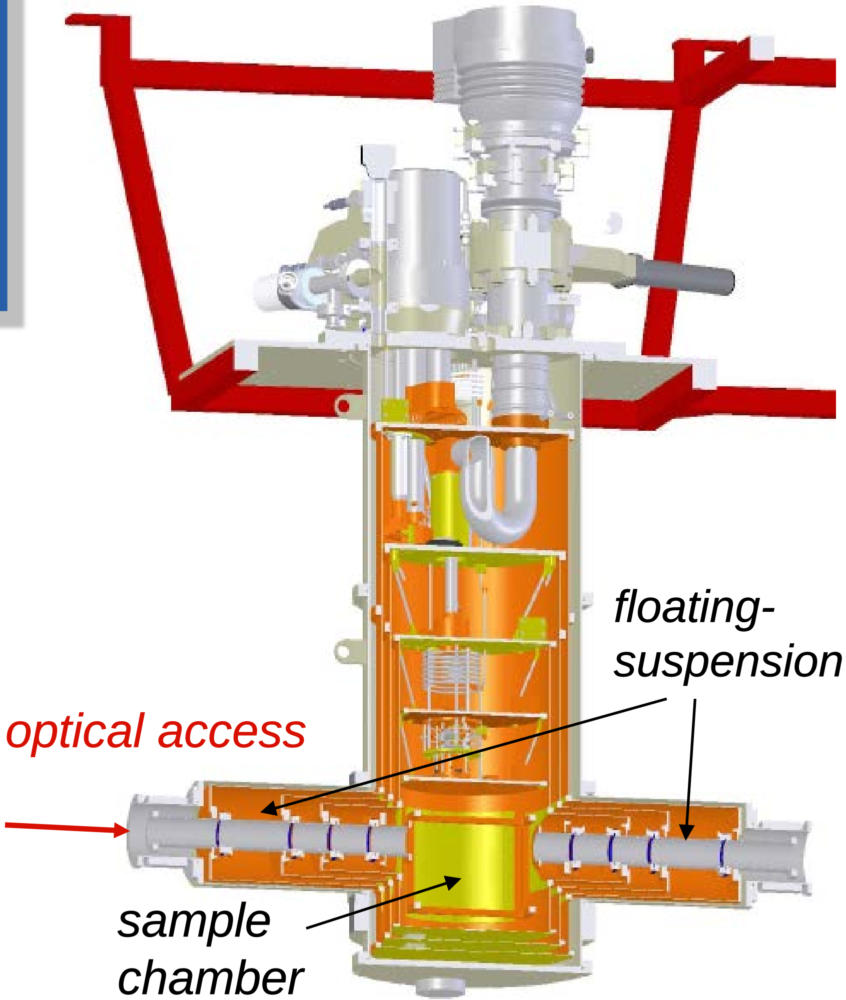

Cryogenic Fiber Interferometer

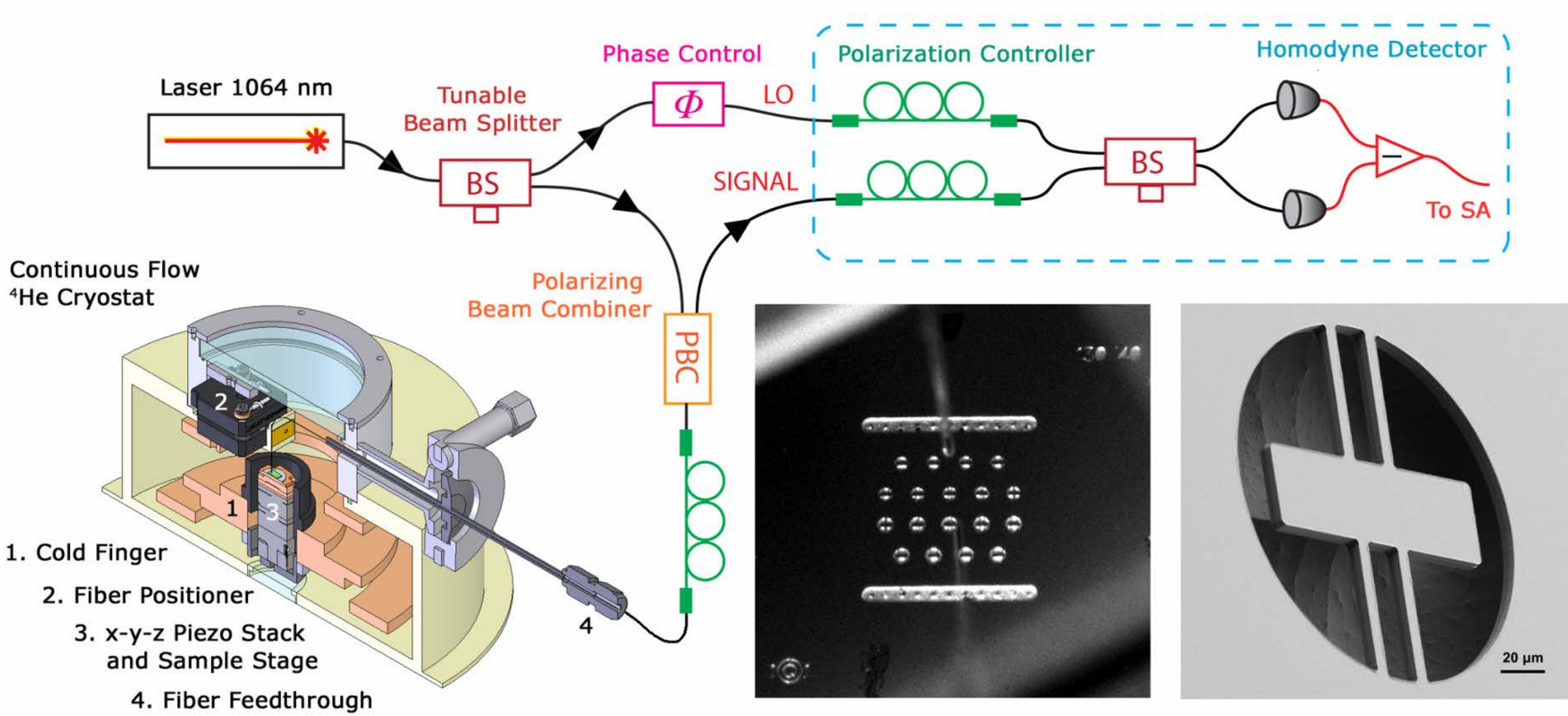

Chip in Cryostat

Resonator Micrograph

- All-fiber setup, continuous flow ^{4}He cryostat for sample chamber
- Operation from 300 K to 20 K, minimum pressure of 2.5×10^{-7} millibar
- Homodyne detection yields sensitivity of 6×10^{-12} m/$\sqrt{\text{Hz}}$ (near 2 MHz)

Compiled Results: R = 116 µm

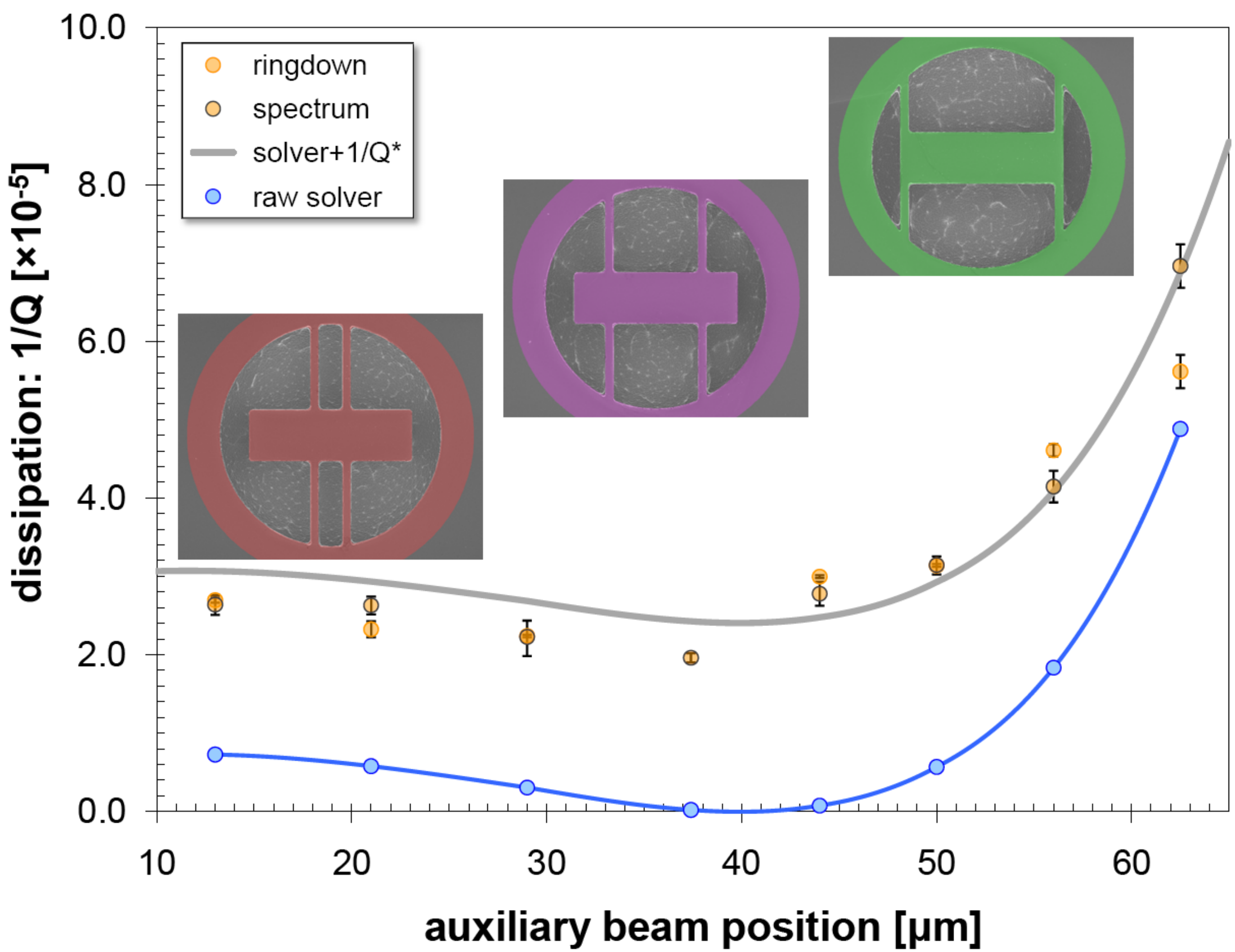

- Inset images: micrographs of resonators with CAD overlay
- Simultaneously fitting all devices
  - both radii (x 2)
  - two chips
- Free parameter
  - 1/Q* (offset) for background dissipation

G. D. Cole and I. Wilson-Rae, et al., Nature Communications 2, 231 (2011)

Compiled Results: R = 131 µm

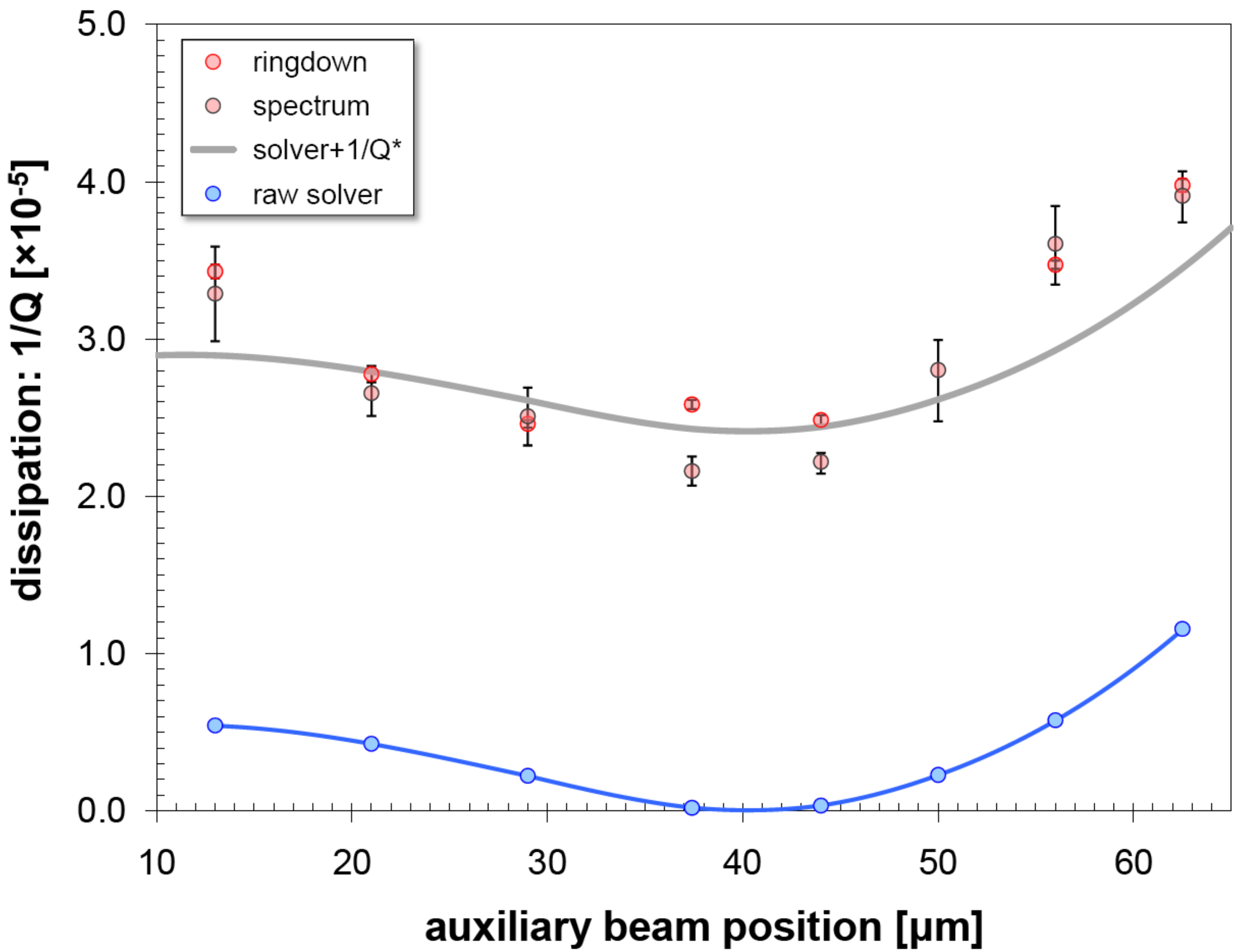

- 1/Q* offset of 2.41×10^{-5} for optimal fitting
  - material related damping mech.
- Substrate props:
  - grade 2 Ti
  - E: 116 GPa
    ρ: 4540 kg/m^3
- Excellent match
  - single free parameter

Mechanical Loss Mechanisms

Four key factors contribute to total dissipation

$$\boxed{\frac{1}{Q_{total}} = \frac{1}{Q_{fluidic}} + \frac{1}{Q_{thermoelastic}} + \frac{1}{Q_{materials}} + \frac{1}{Q_{anchor}}}$$

First two mechanisms are well understood:

1. Fluidic: results from air flow around moving structure or squeeze-film effects from trapped gases

2. Thermoelastic: strain driven thermal gradient dissipated via irreversible heat conduction

1: Langlois (1962), Griffin (1966), Blech (1983) | 2: Zener (1937), Lifshitz (2000), Duwel (2005)

Mechanical Loss Mechanisms

Four key factors contribute to total dissipation

$$\boxed{\frac{1}{Q_{total}} = \frac{1}{Q_{fluidic}} + \frac{1}{Q_{thermoelastic}} + \frac{1}{Q_{materials}} + \frac{1}{Q_{anchor}}}$$

Remaining mechanisms require further investigation:

3. Materials: intrinsic to the specific microstrucutre, e.g. two-level fluctuators in amorphous materials (SiO_2)

4. Anchor: acoustic transmission from the resonator into the supporting medium (i.e. phonon tunneling)

(3) Mihailovich & MacDonald (1995), Yasumura (2000) | (4) Wilson-Rae (2008)

Modal Analysis (Measured and FEM)

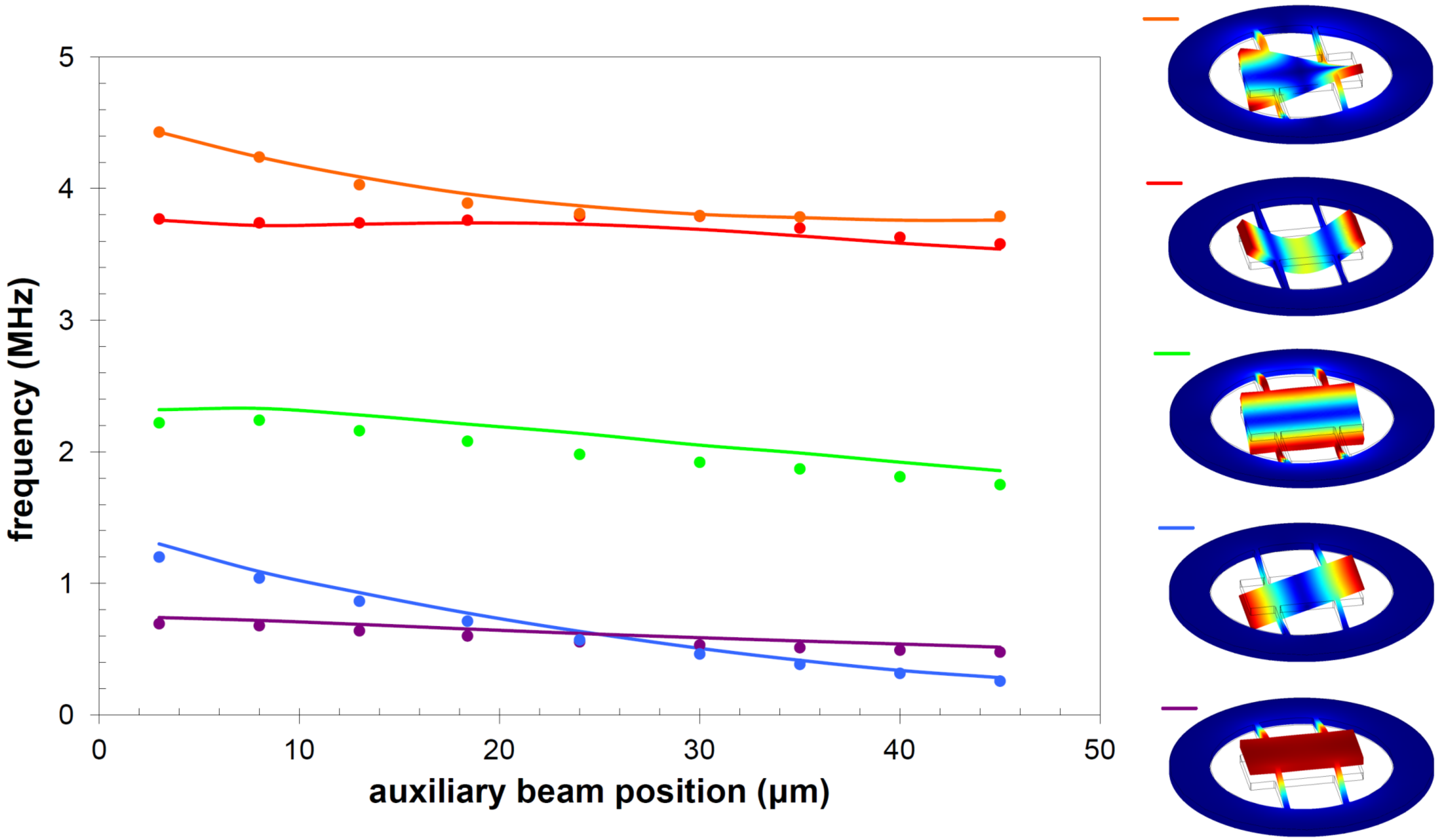

Mode Tomography System

Updates:
1) focused probe beam
2) encoded stage

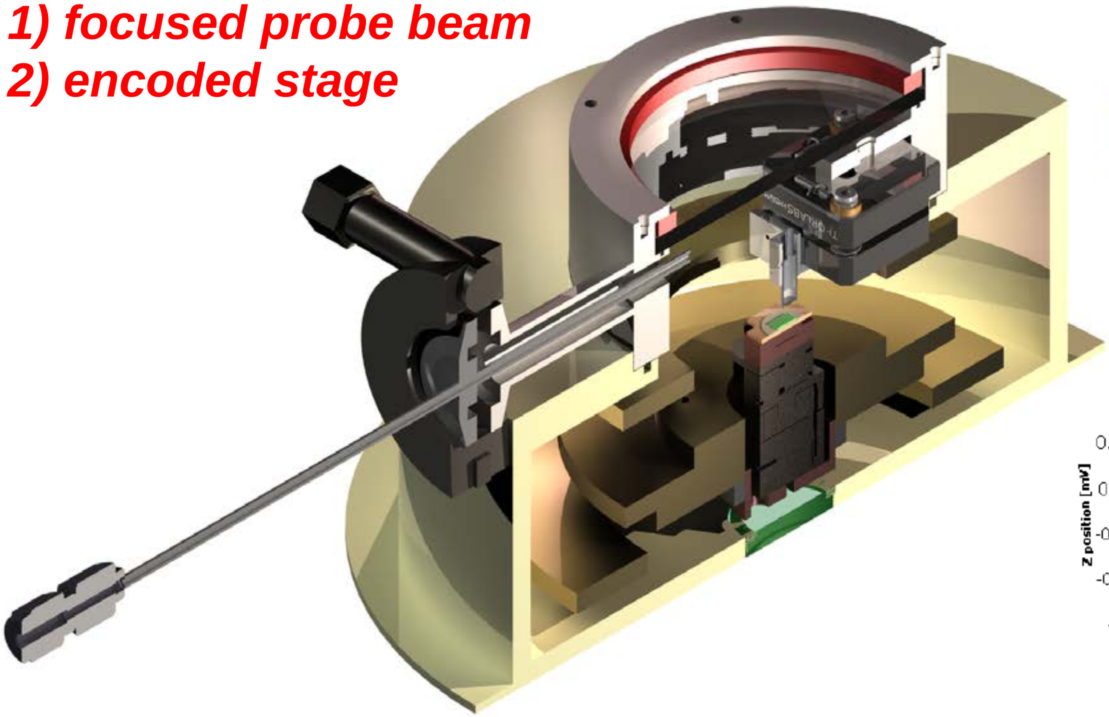

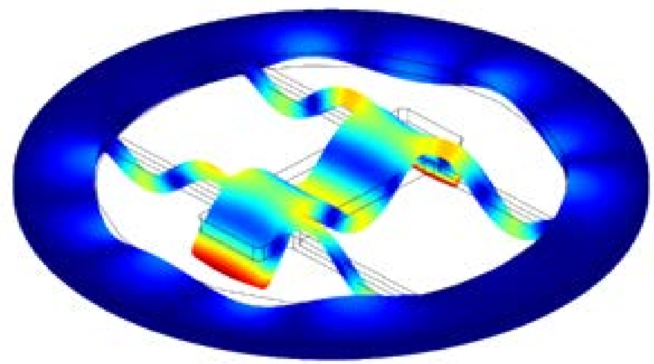

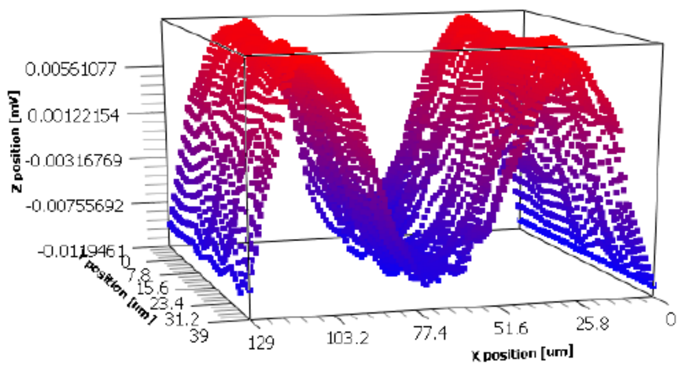

- Eigenmodes are selectively excited with a narrow driving frequency
- Fiber focuser (10 µm Ø) allows for pointwise probing of displacement
- Encoded attocubes yield position data for modal analysis

Dissipation Characterization

Resonance

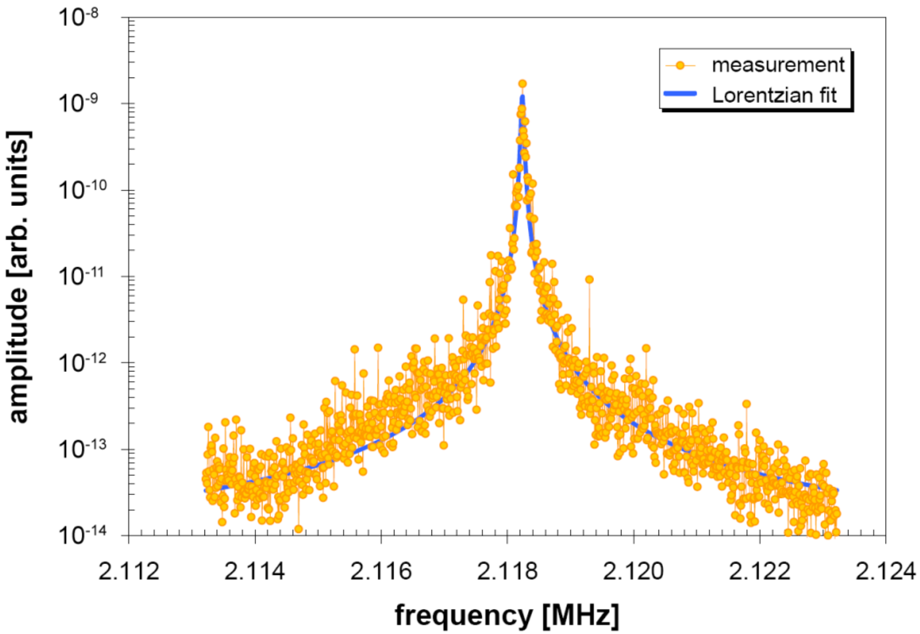

Ringdown

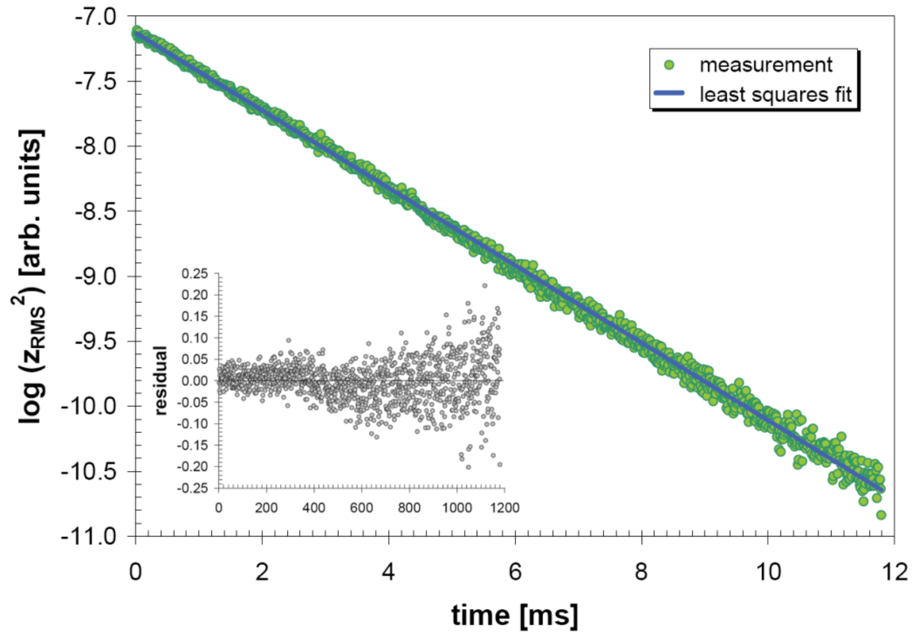

- Two methods for Q determination: white noise and resonant driving
  - white noise excites all modes simultaneously, Lorentzian fitting for Q
  - coherent drive and cessation for free-ringdown response, exponential fit

G. D. Cole and I. Wilson-Rae, et al., Nature Communications 2, 231 (2011)

Phonon Tunneling Concept

Mechanical Resonator
(Phononic Cavity)

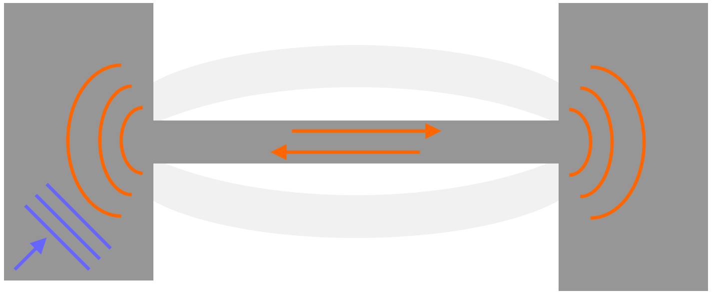

Optical Resonator
(Photonic Cavity)

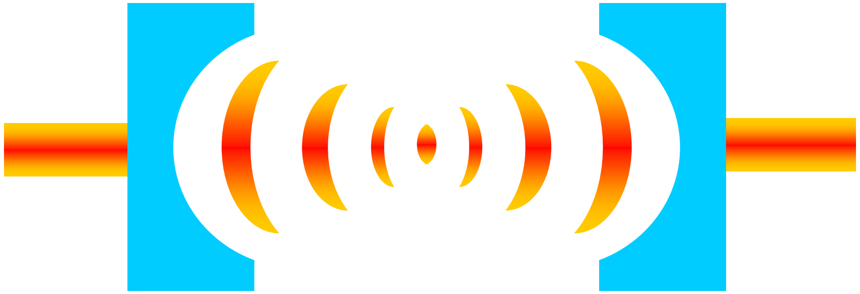

- Goal: calculate scattering modes of mechanical resonator
- Analogy: resonator as a mechanical Fabry-Perot interferometer
  - transmission and reflection of phonons at 3D-1D junction
- Resonator → phononic waveguide: 4 branches lacking infrared cutoff
  - compression (c), torsion (t), vertical (v), and horizontal (h) bending
- Phononic modes of resonator/substrate calculated via elasticity theory
  - inverse aspect ratio (d/L) yields natural small parameter

I. Wilson-Rae, Phys. Rev. B 77, 245418 (2008)

Phonon Tunneling Q-Solver

$$\frac{1}{Q} = \frac{\pi}{2\rho_s \rho_R \omega_R^3} \int_q \left| \int_S \mathrm{d}\bar{S} \cdot \left(\boldsymbol{\sigma}_q^{(0)} \cdot \bar{u}'_R - \boldsymbol{\sigma}'_R \cdot \bar{u}_q^{(0)} \right) \right|^2 \delta[\omega_R - \omega(q)]$$

- Coupling of the free modes of the substrate and suspended resonator
  - applying Fermi's Golden Rule to phonon decay with the interaction Hamiltonian between the resonator volume and supports
- Calculation enabled by a standard eigenfrequency analysis via FEM
  - resonator mode and stress distribution via COMSOL
  - cylindrical modes assumed for support; substrate modelled as elastic half-space

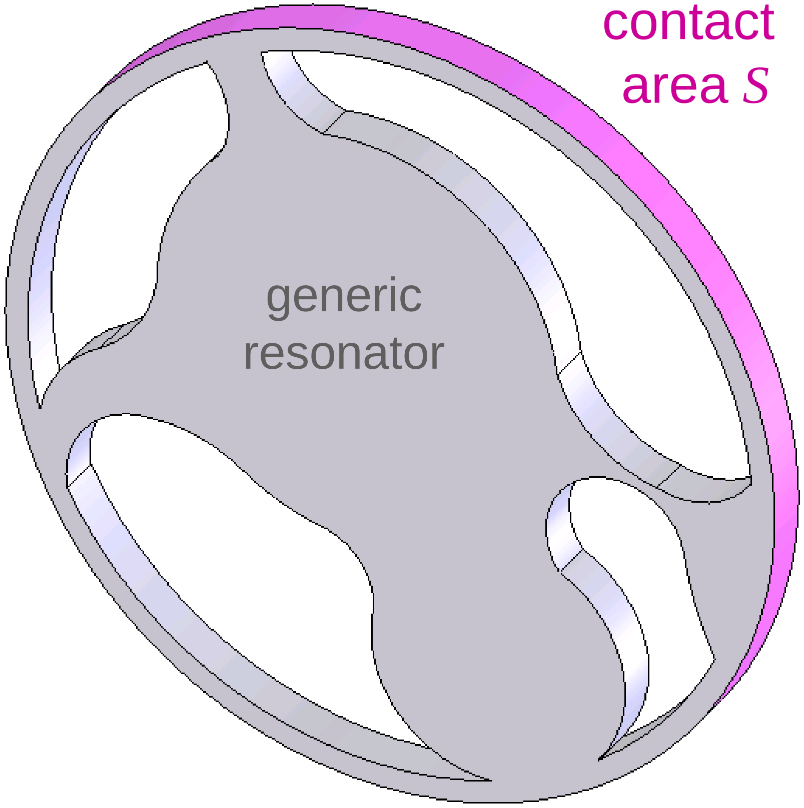

I. Wilson-Rae, Phys. Rev. B 77, 245418 (2008)

Initial Verification of Numerical Solver

- Simple beam geometries tested to ascertain errors in numerical simulation
  - plot: results for 1x1 μm^2 bridges with aspect ratios from 15:1 to 40:1
- Compares well with analytical expressions developed previously
  - FEM-derived Q values scale as length^5 for doubly-clamped beams
  - we record a maximum error of 20% for this initial test (failure of the weak coupling approx.)

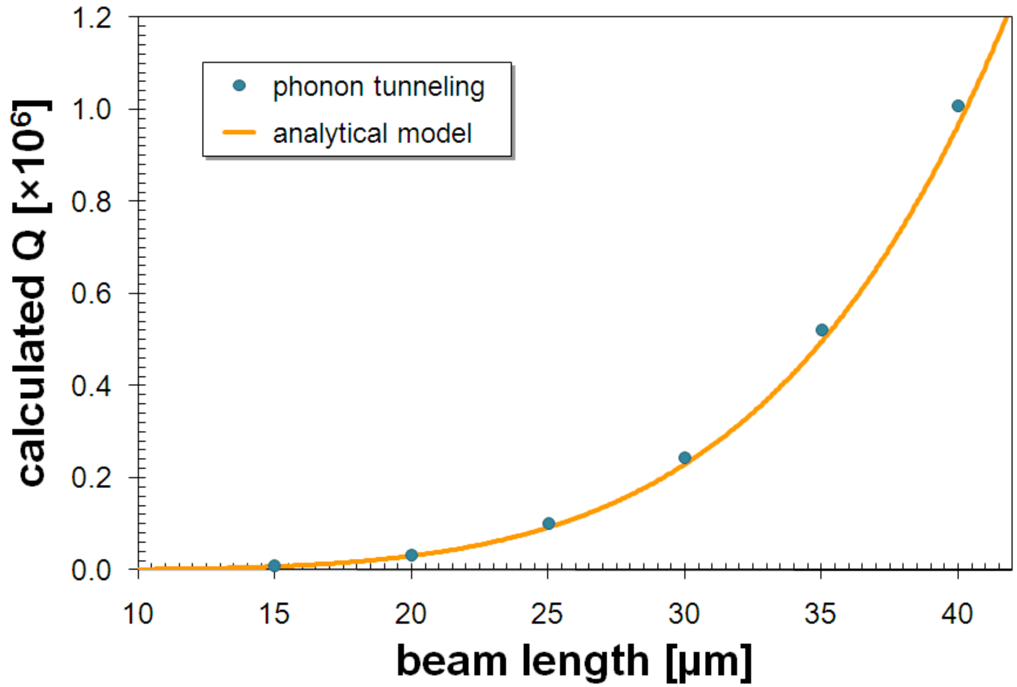

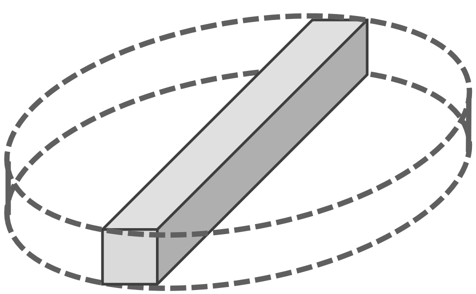

$$Q_{c-c} = \frac{0.92\, L^5}{\pi^4 \mathrm{wt}^4}$$

D. M. Photiadis, et al., Appl. Phys. Lett. (2004) | I. Wilson-Rae, Phys. Rev. B (2008)

Mode Identification

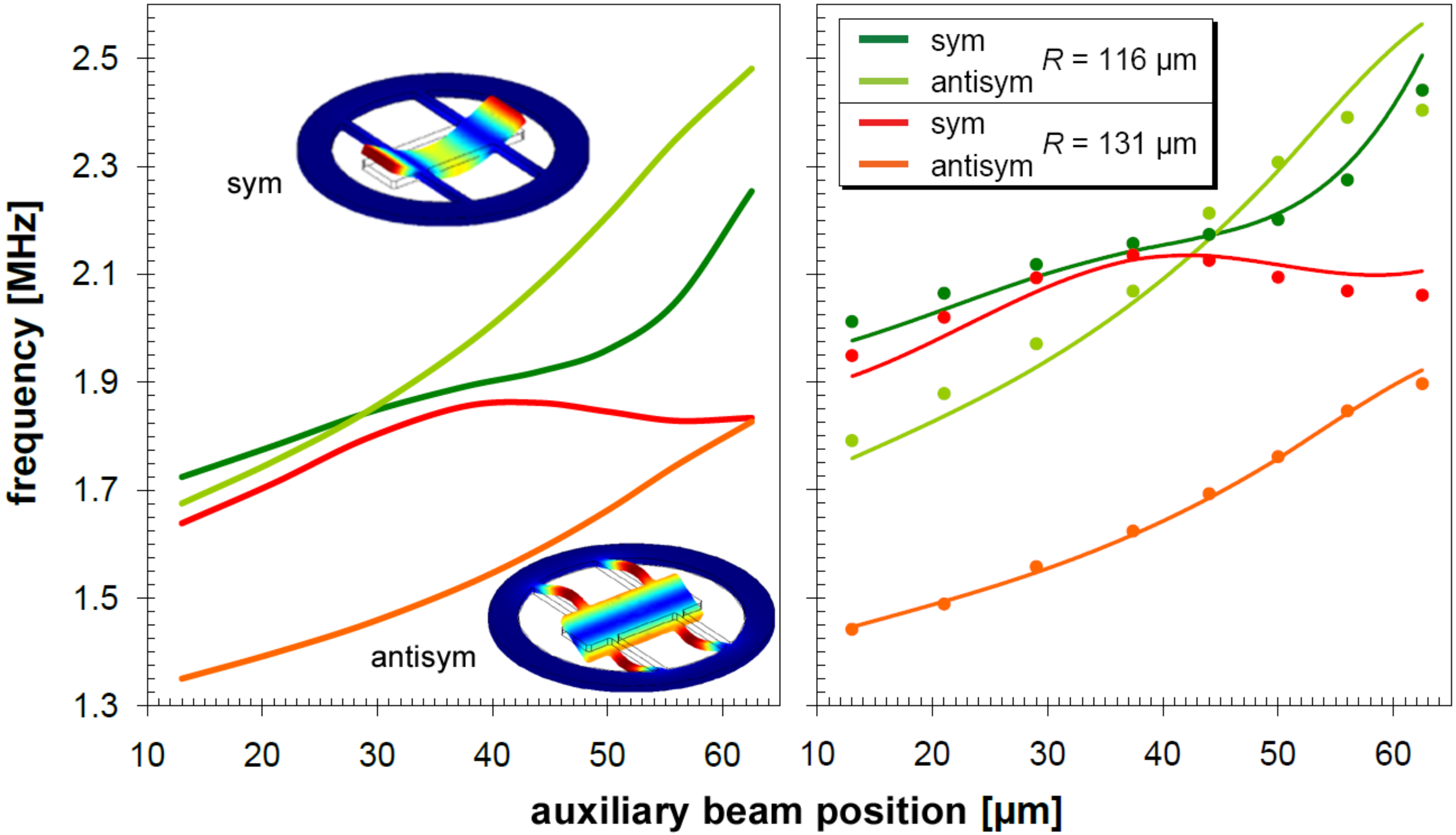

- FEM accurately captures geometric dependence of the resonances

Mode Identification

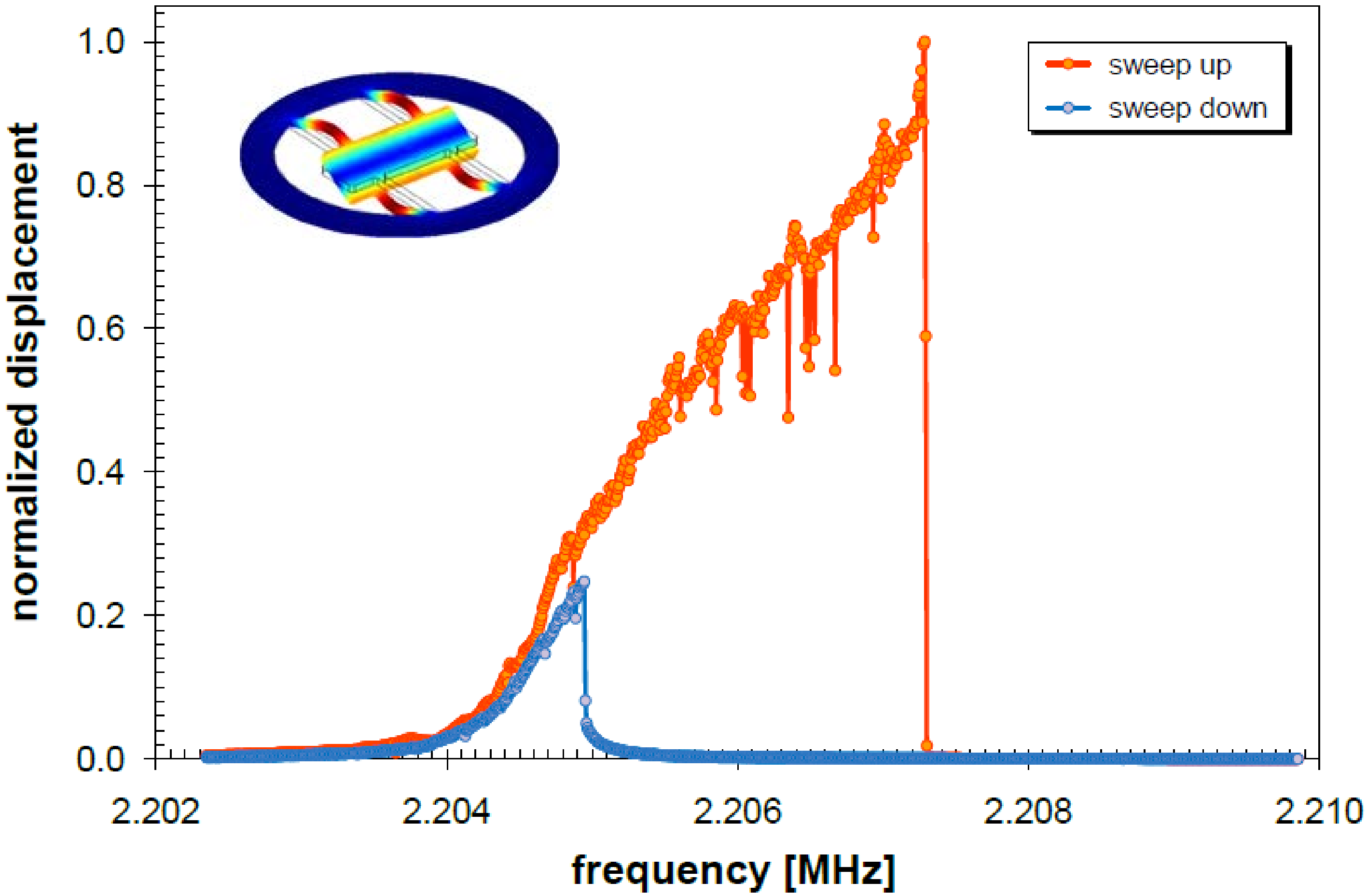

- Antisymmetric mode displays hardening-spring Duffing response

Experimental Parameters

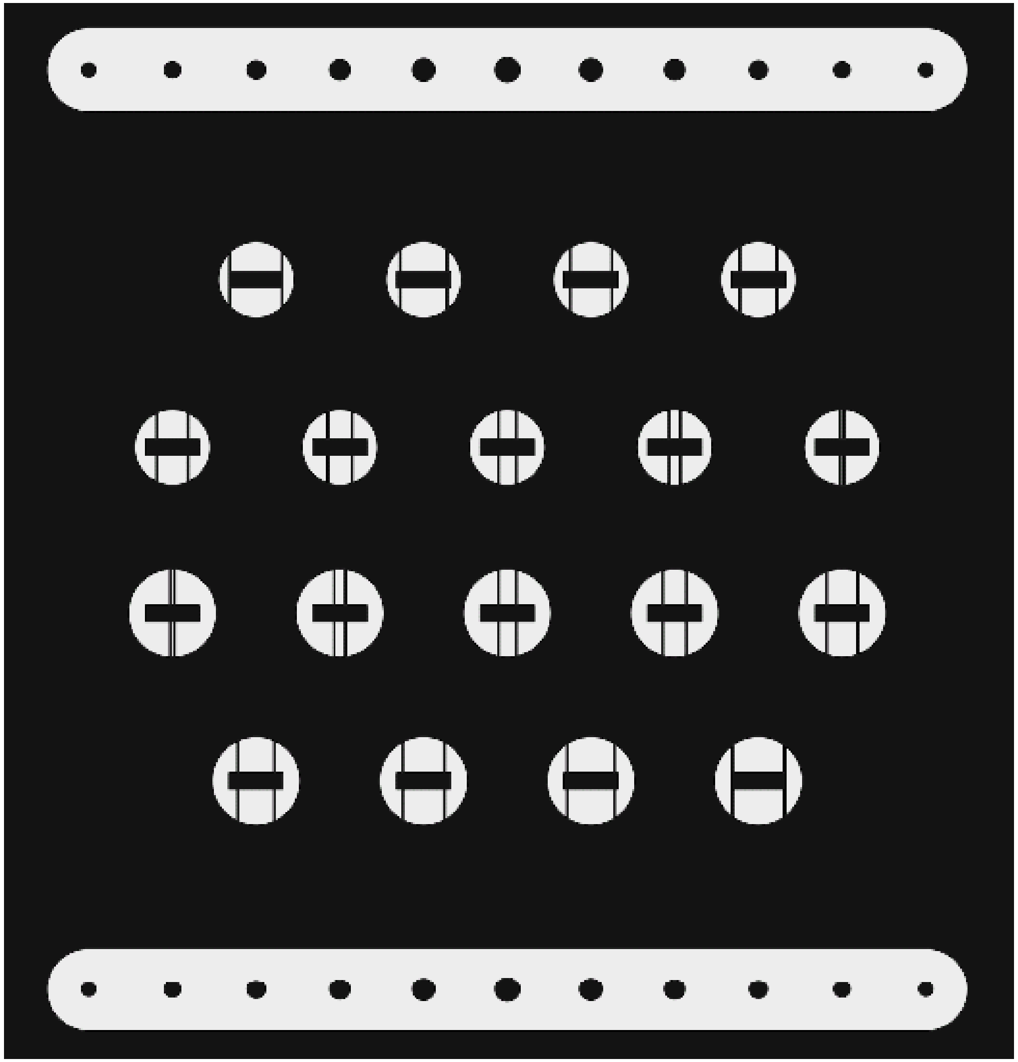

- Fixed central resonator dimensions: 130 x 40 μm
- Varying auxiliary beam attachment points (8)
  - 13, 21, 29, 37.4, 44, 50, 56, and 62.5 μm
  - aux. beams sample resonator mode shape
- Two distinct outer radii of 90 and 105 μm
  - investigate Q-variation in aux. beam length
- Undercut process monitoring structures

Heteroepitaxial Monocrystalline DBR

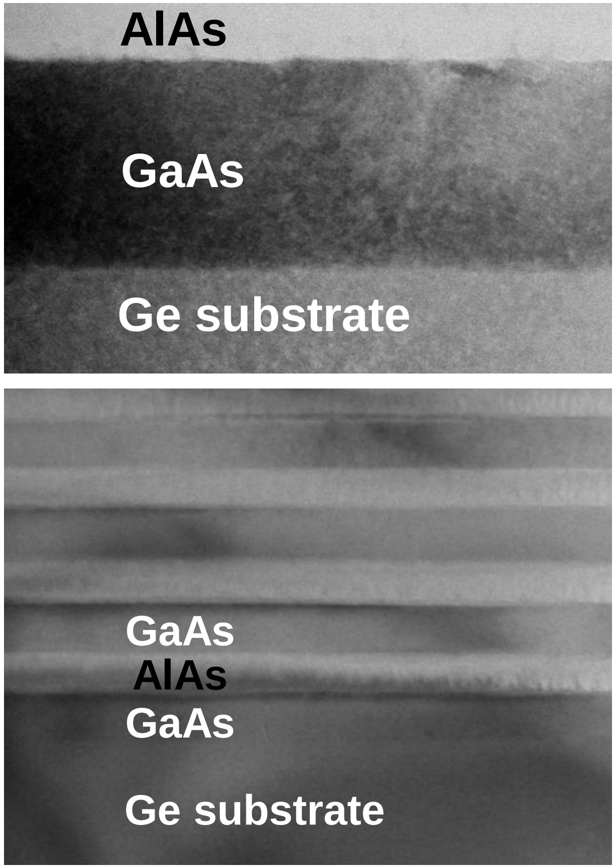

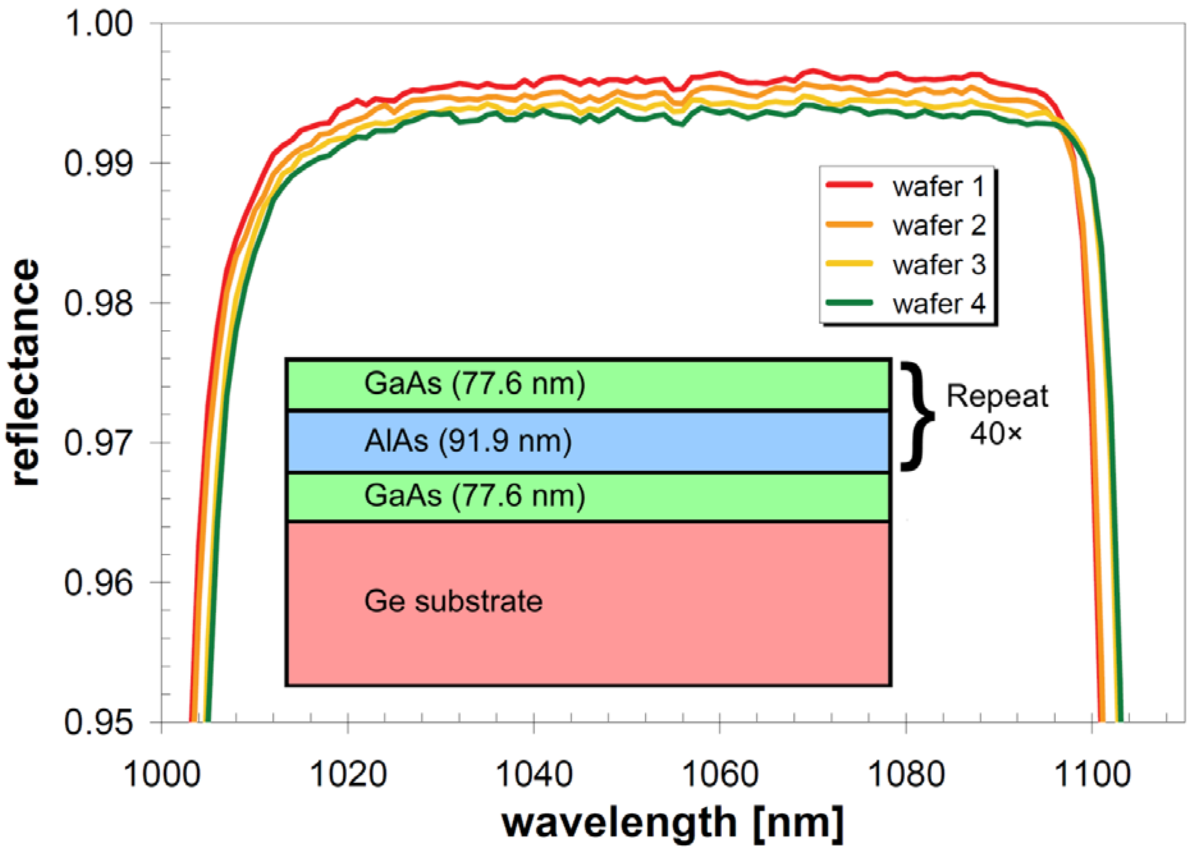

- 40-period GaAs/AlAs crystalline multilayer grown on a Ge substrate
  - Ge sacrificial material allows for increased flexibility in processing
- Surface roughness due to lattice mismatch limits reflectance (99.87%)

Crystal Growth Details

- Thomas Swan/AIXTRON low-pressure MOCVD reactor with a close-coupled showerhead configuration
- 2” diameter, 375-um thick, epi-ready (100) Ge substrates, offcut 6° toward the [011] direction
- Offcut substrate necessary to inhibit the formation of anti-phase boundaries (APBs)
- N_2 is used as the carrier gas and chamber pressure is maintained at 100 Torr during crystal growth

S. M. Ting and E. A. Fitzgerald, “Metal-organic chemical vapor deposition of single domain GaAs on Ge/Ge_xSi_{1-x}/Si and Ge substrates,” *Journal of Applied Physics* vol. 85, 2618, 2000.

AlGaAs on Ge Crystal Quality

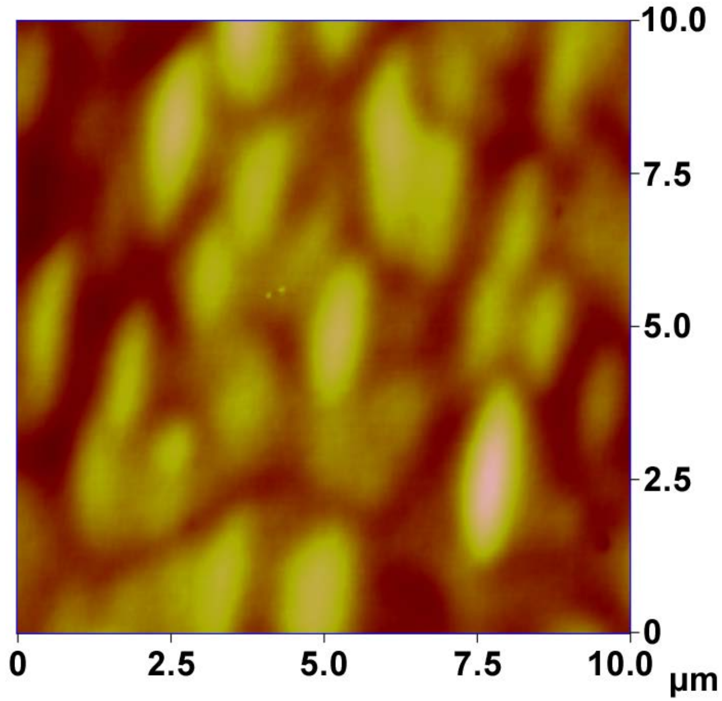

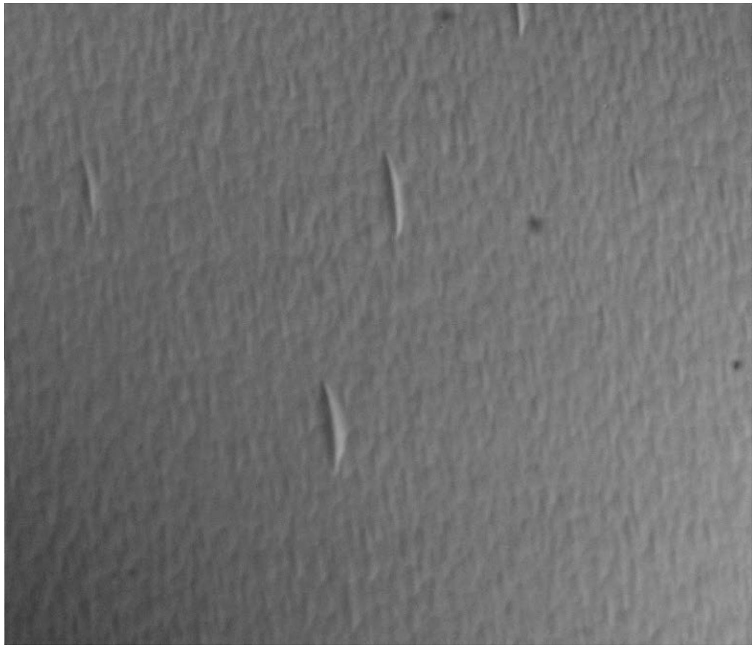

- DBR exhibits significant roughness (>30 Å measured via AFM)
  - interfacial misfit dislocations, residual anti-phase boundaries (APBs)
- Ge and GaAs lattice mismatch is small but significant (~ 0.3%)
  - calculated critical thickness of GaAs on Ge is approximately 1 μm
  - In and P incorporation can be used to achieve lattice matching to Ge

Microfabricated Optomechanics Gen I

Laser Ablation

with Dieter Bäuerle (Linz)
and Keith Schwab (Cornell)

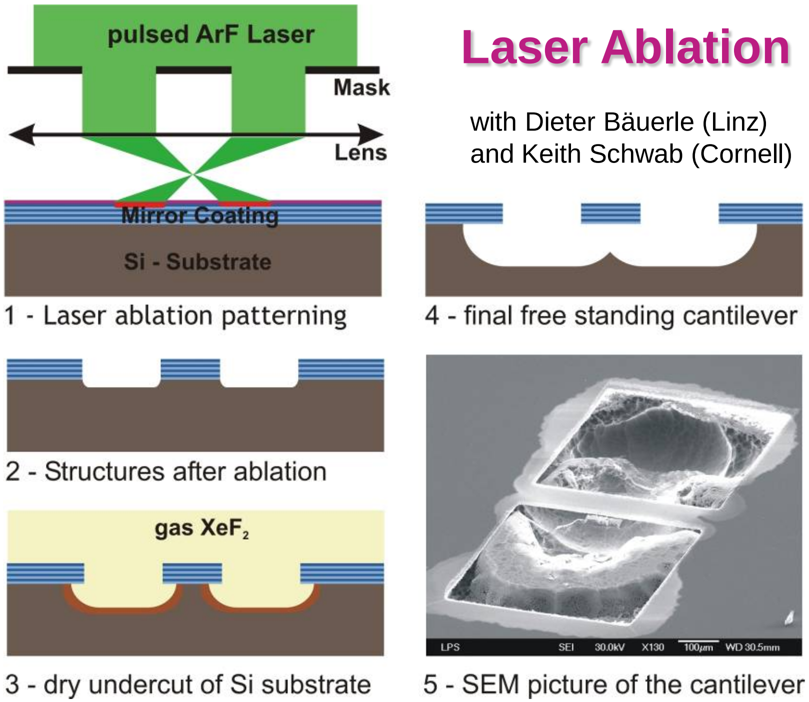

free-standing HR coating (TiO_2/SiO_2)
dimensions: 520 x 120 x 2.4 μm^3
Reflectivity > 0.998, Q ~ 10,000

H.R. Böhm, S. Gigan, G. Langer, J. Hertzberg, F. Blaser, D. Bäuerle, K. Schwab, A. Zeilinger, M. Aspelmeyer, Appl. Phys. Lett. 89, 223101 (2006)

Dry Etching

with Keith Schwab
(Cornell)

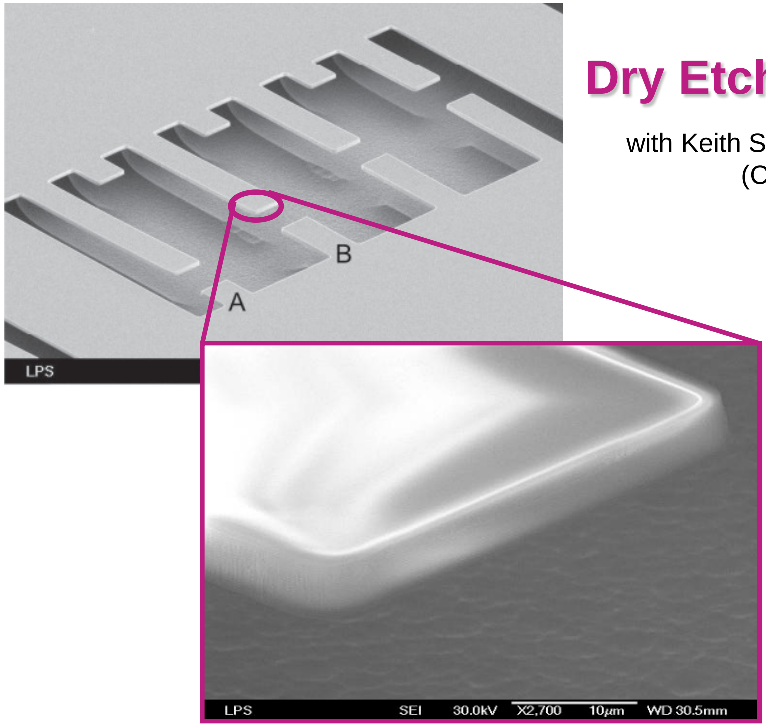

free-standing HR coating (Ta_2O_5/SiO_2)
dimensions: 250 x 50 x 6 μm^3
Reflectivity > 0.9999, Q ~ 2,000

S. Gröblacher, S. Gigan, H. Böhm, A. Zeilinger, M. Aspelmeyer, Eur. Phys. Lett. 81, 54003 (2008)

Microfabricated Optomechanics Gen II

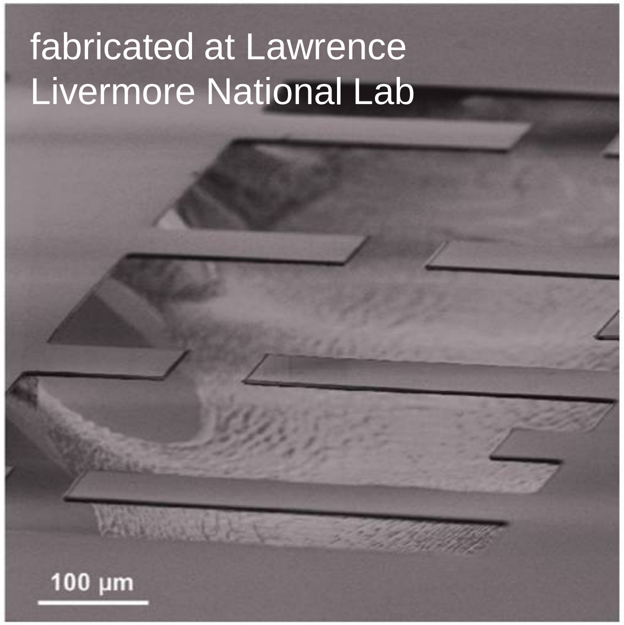

Single Crystal Bragg Mirrors

with G. Cole (LLNL)

free-standing epitaxial AlGaAs DBR
dimensions: 100s x 50 x 5.5 μm^3
Reflectivity > 0.9998, Q ~ 10^4 (κ/ω_m~0.2)

G. D. Cole, S. Gröblacher, K. Gugler, S. Gigan, M. Aspelmeyer, Appl. Phys. Lett. 92, 261108 (2008)

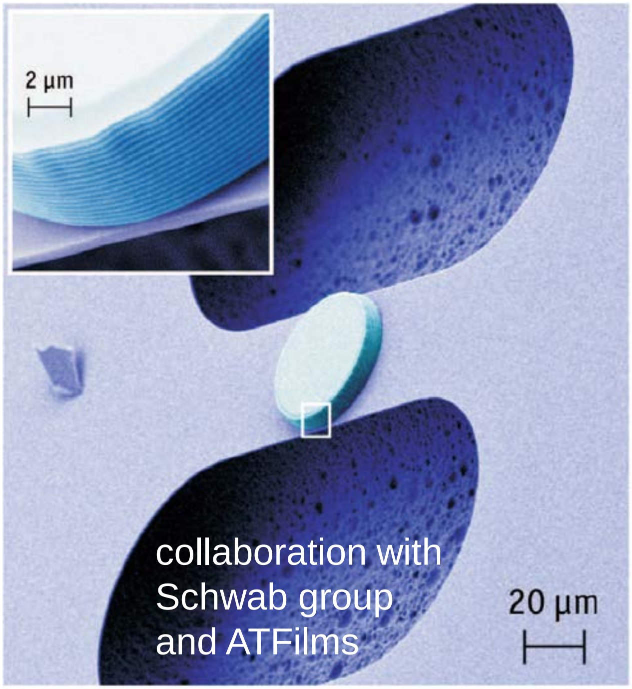

Hybrid SiN_x & Ta_2O_5/ SiO_2

with K. Schwab and R. Lalezari

dielectric mirror pad (Ta_2O_5/SiO_2) on SiN_x
dimensions: 100s x 50 x 6 μm^3
Reflectivity > 0.9999, Q ~ 10^4 (κ/ω_m~0.2)

S. Gröblacher, J. B. Hertzberg, M. R. Vanner, G. D. Cole, S. Gigan, K. C. Schwab, and M. Aspelmeyer, Nature Physics 7, 485 (2009)

Completed Free-Free Resonators

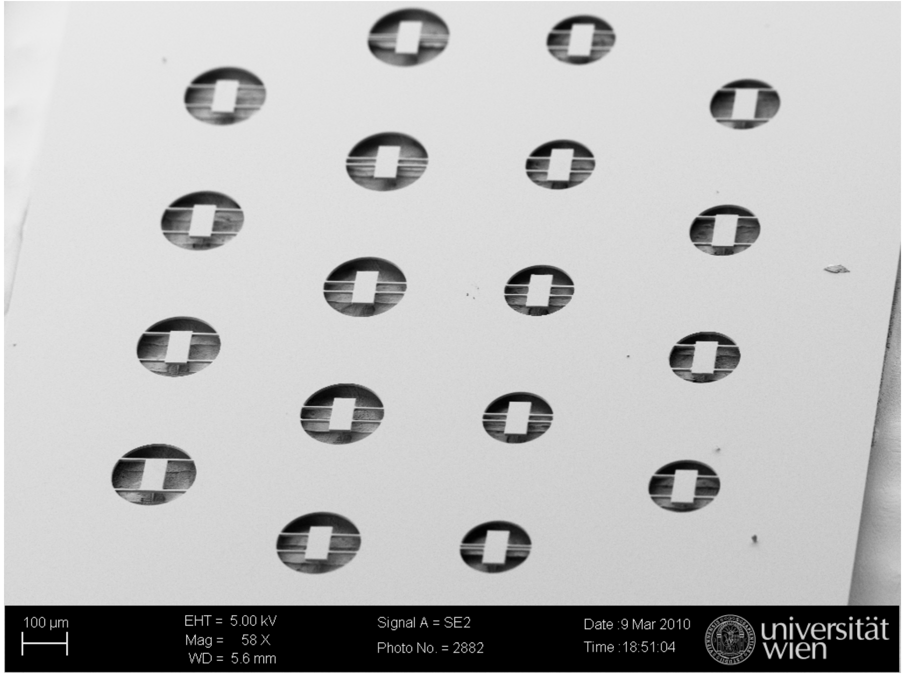

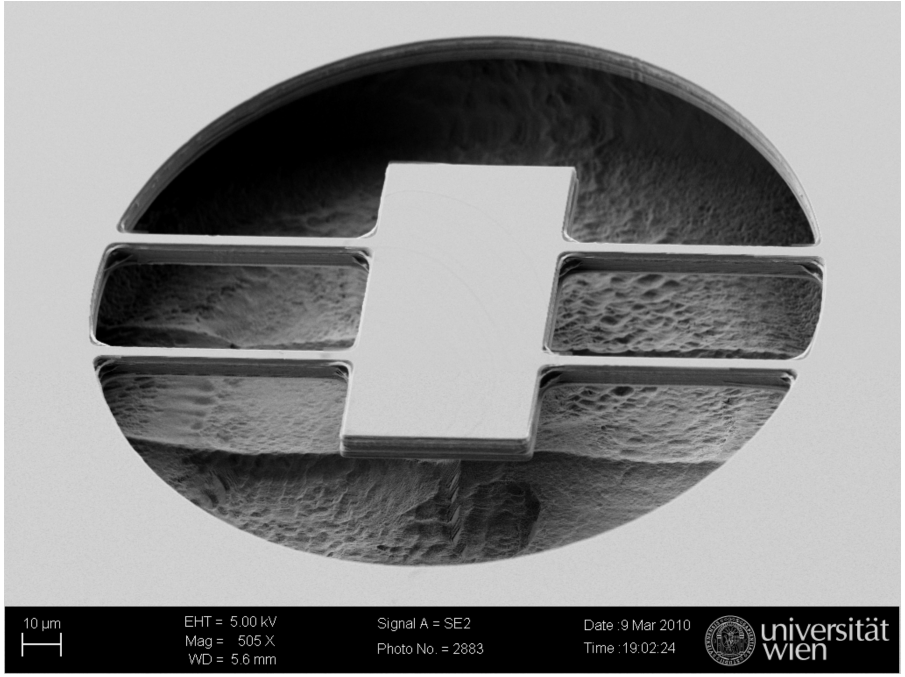

- Single-mask bulk micromachining process, $SiCl_4/N_2$ ICP for DBR etch
- Selective etching of binary GaAs over ternary $Al_{0.12}Ga_{0.88}As$ for release